Study of X-ray flares from the wind-fed X-ray binaries

Maksat Satybaldiev

Astro and Theory Seminar, NTNU
07/11/2023

Pic credits: DALL-E 2

X-ray Binaries

NS/BH + Donor Star

Low Mass X-ray Binaries (LMXBs)

$M_C \lesssim 1 M_\odot$

old: $\sim 10^9$ years

(bursters, symbiotic binaries…)

High Mass X-ray Binaries (HMXBs)

$M_C \gtrsim 10 M_\odot$

young: $\lesssim 10^7$ years

(SgXBs, BeXBs, SFXTs…)

Disk-fed
(RLOF)

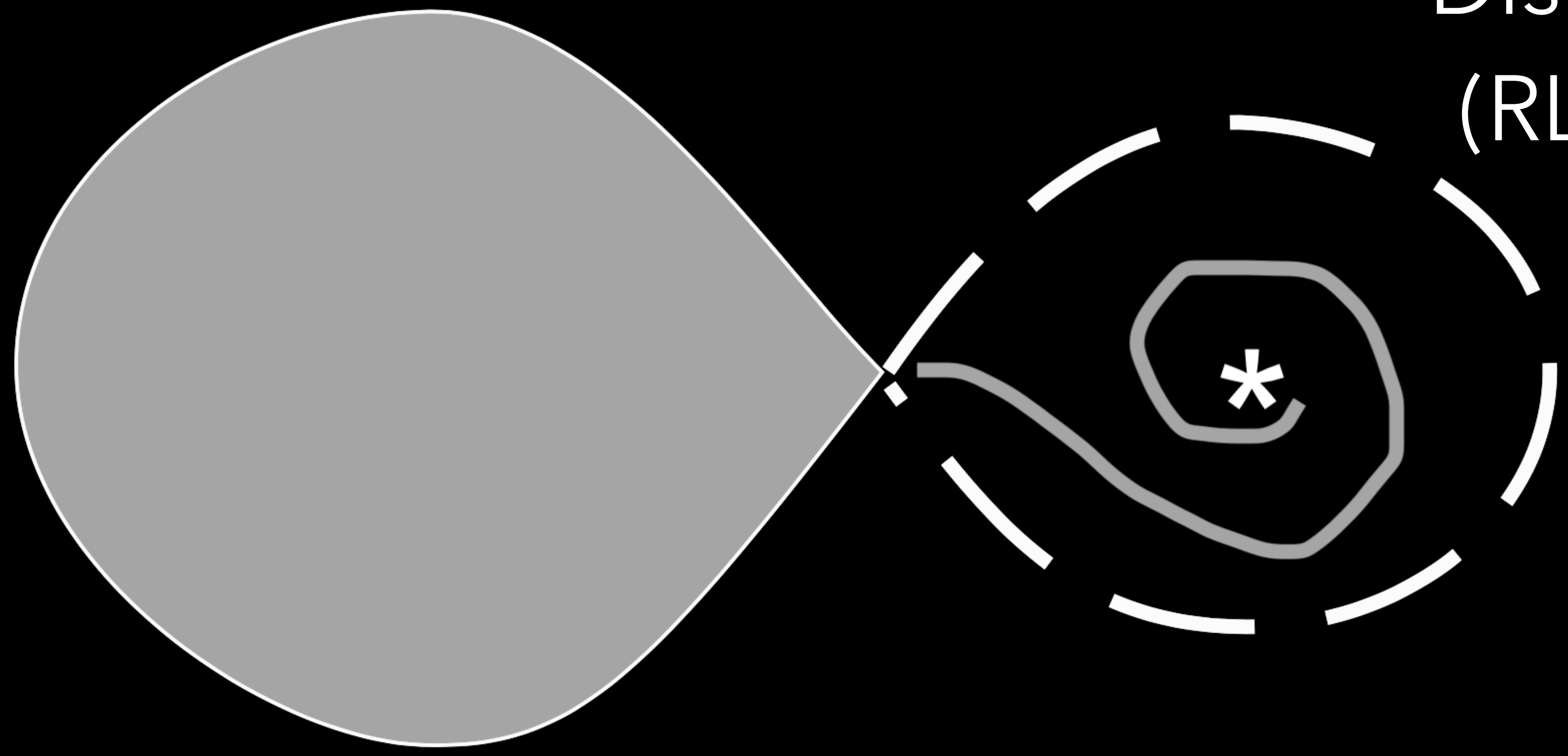

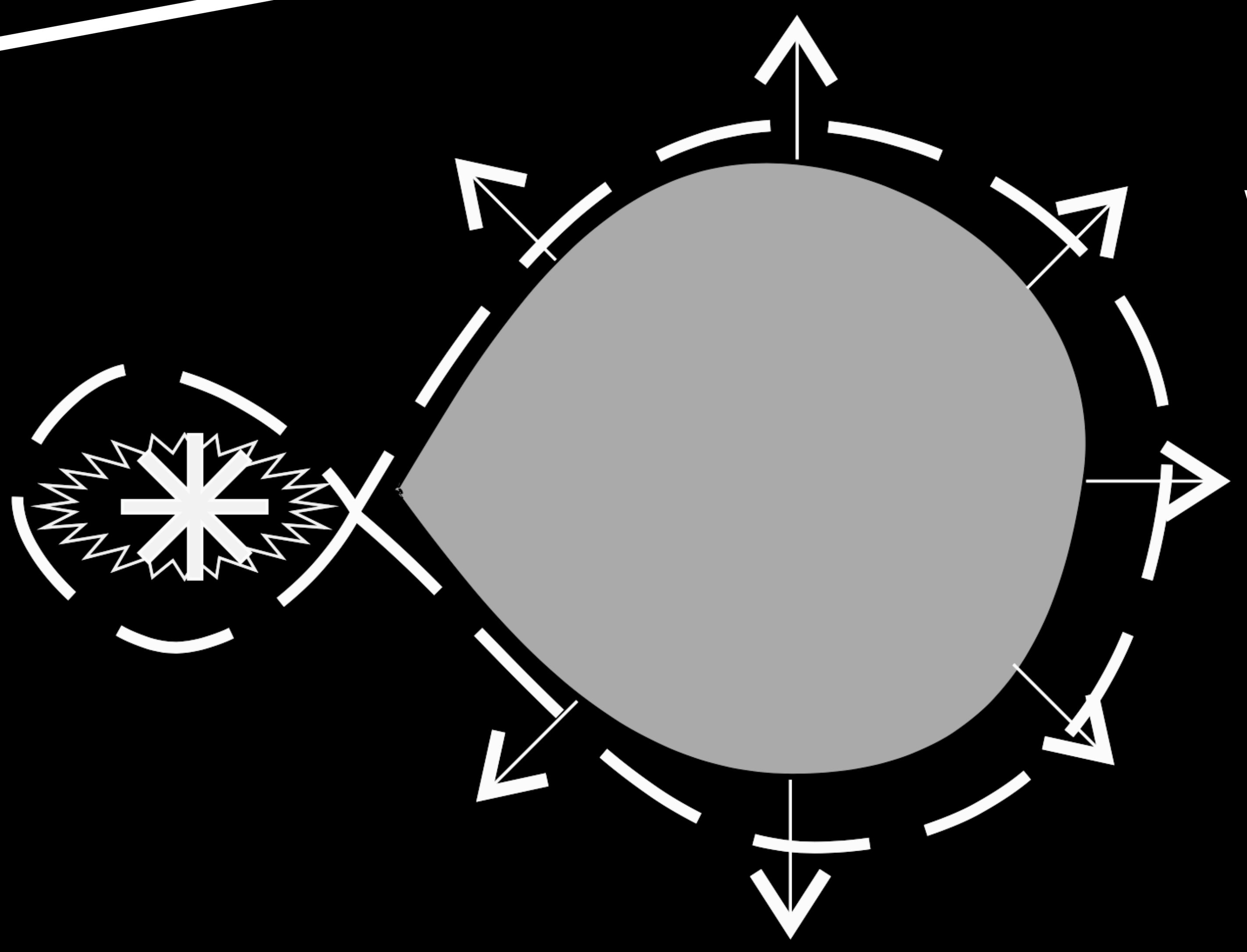

Wind-fed

- IGR J16195-4945 (SFXT)
- 3A 1954+319 (RSG XB)

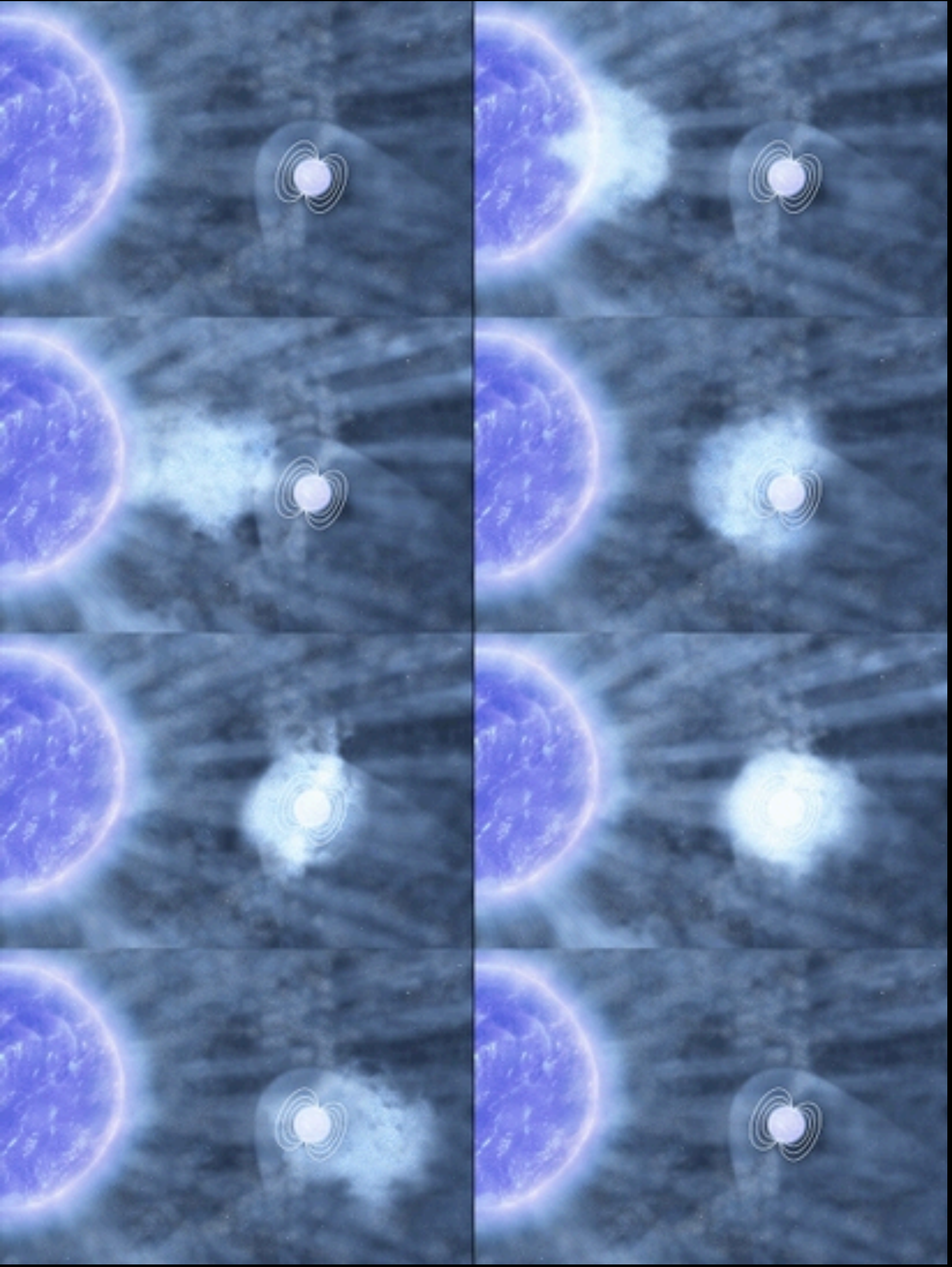

Credits: ESA/AOES Medialab

SFXT - Supergiant Fast X-ray Transient

- HMXB: compact object accretes the clumpy wind from supergiant companion
- Bright sporadic X-ray flares: dynamic range ≥ 10, duration ~1000 s, duty cycle $\lesssim$ 5%
- Average luminosity $L \lesssim 10^{34}$erg s^{-1}
- Possible models:
  - extremely clumpy winds (in't Zand 2005): clump masses $\sim 10^{21} - 10^{23}$ g,
  - centrifugal or magnetic gates (Grebenev 2008; Bozzo et al. 2008): $B \sim 10^{12}$ G, P_{spin} ~ 10 s or $B \sim 10^{14}$ G, $P_{spin} \gtrsim 1000$ s,
  - quasi-spherical subsonic settling accretion (Shakura et al. 2012): $L_X \lesssim 4 \times 10^{36}$ erg s^{-1}

X-ray Binaries with Red Supergiant Donor (RSG XBs)

Wind-fed X-ray Binaries

Galactic RSG SgXBs:
3A 1954+319 (Hinkle et al. 2020)
SWIFT J0850.8-4219 (De et al. 2023)
(?) CXO 174528.79-290942.8 (Gottlieb et al. 2020)

IGR J16195-4945

- Discovered by INTEGRAL (Walter et al. 2004)
- Orbital period $P_o = 3.945 \pm 0.005\ d$ (Cusumano et al., 2016)
- Eclipsing HMXB, duration ~3.5% of P_o (Cusumano et al., 2016)
- Blue Supergiant **ON9.7Iab** companion star (Coleiro et al., 2013)
- Distance ~5-15 kpc (Tomsick et al., 2006)

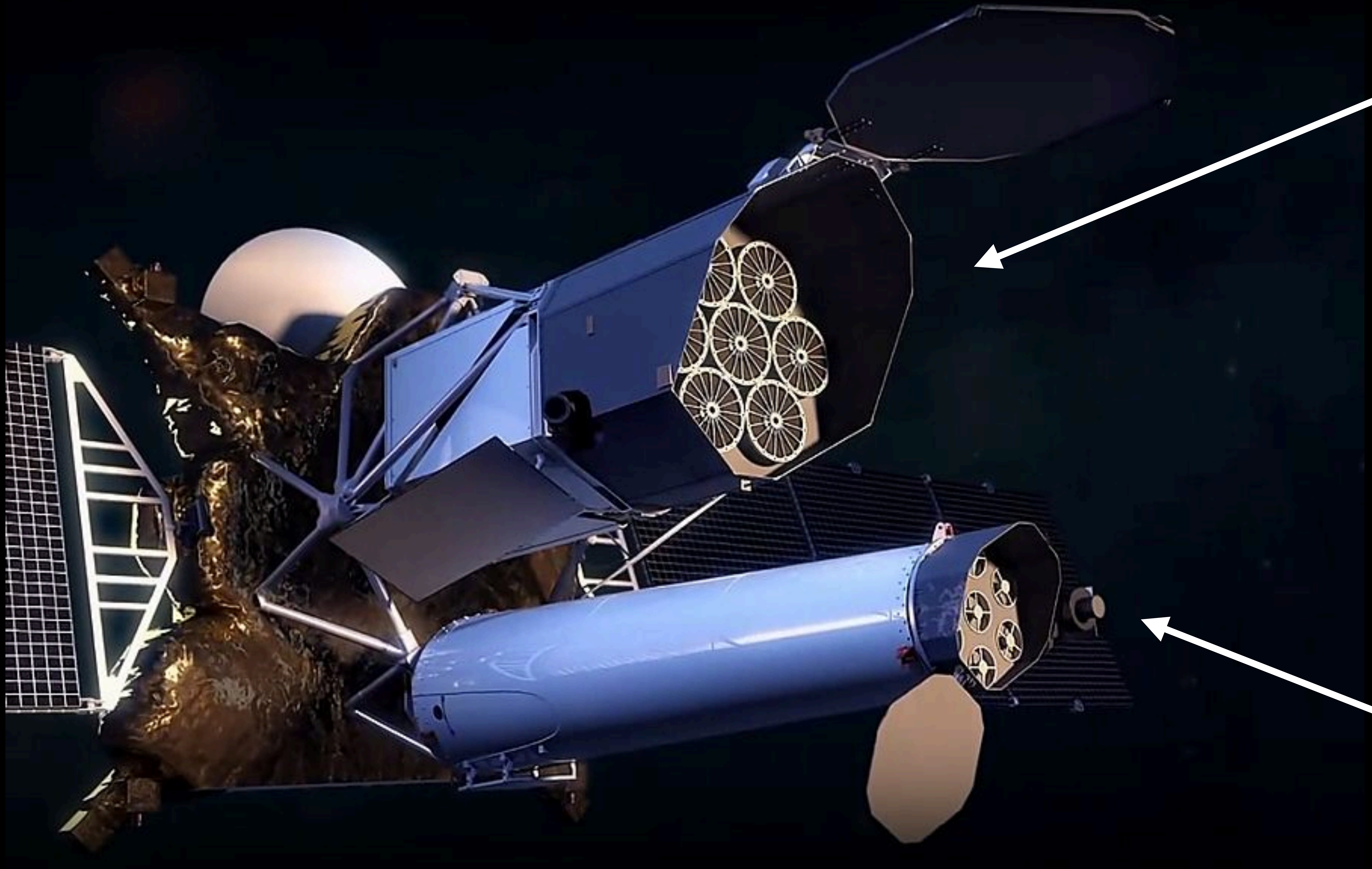

SRG/eROSITA

0.3-11 keV

SRG/ART-XC

4-30 keV

SRG/ART-XC observed IGR J16195-4945 from 2021-03-03 01:42 UTC to 2021-03-04 01:40 UTC

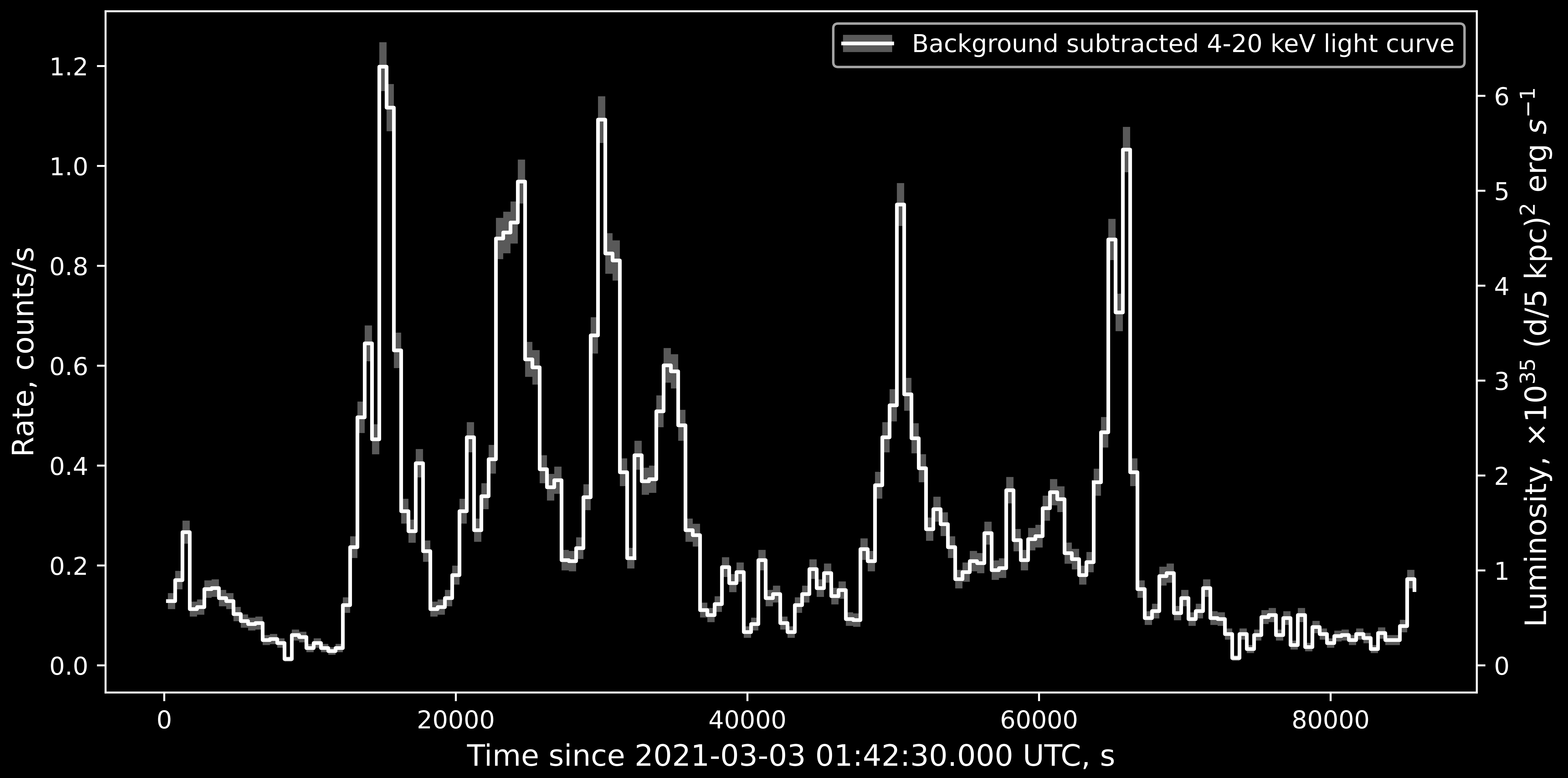

Epoch Folding

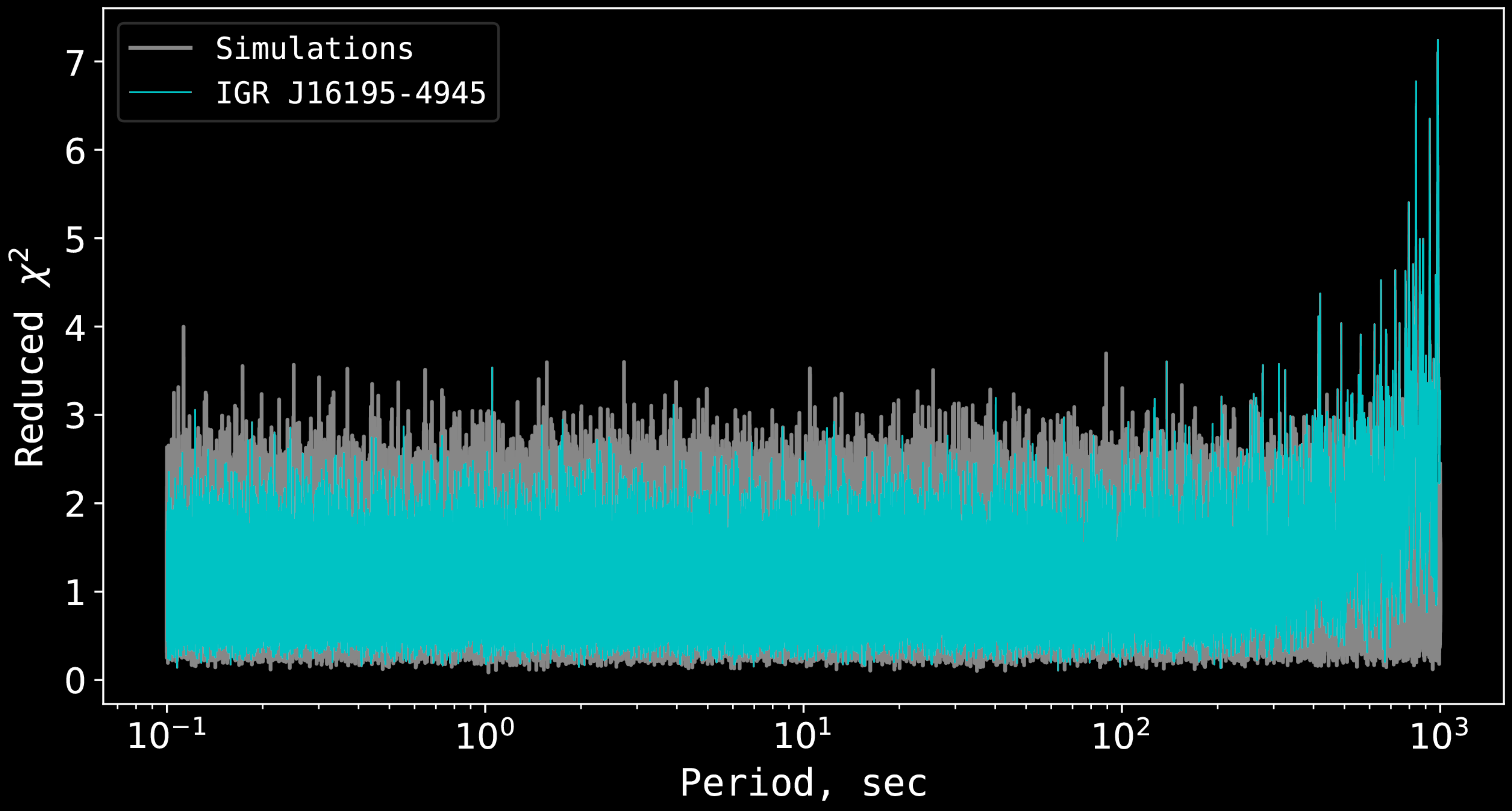

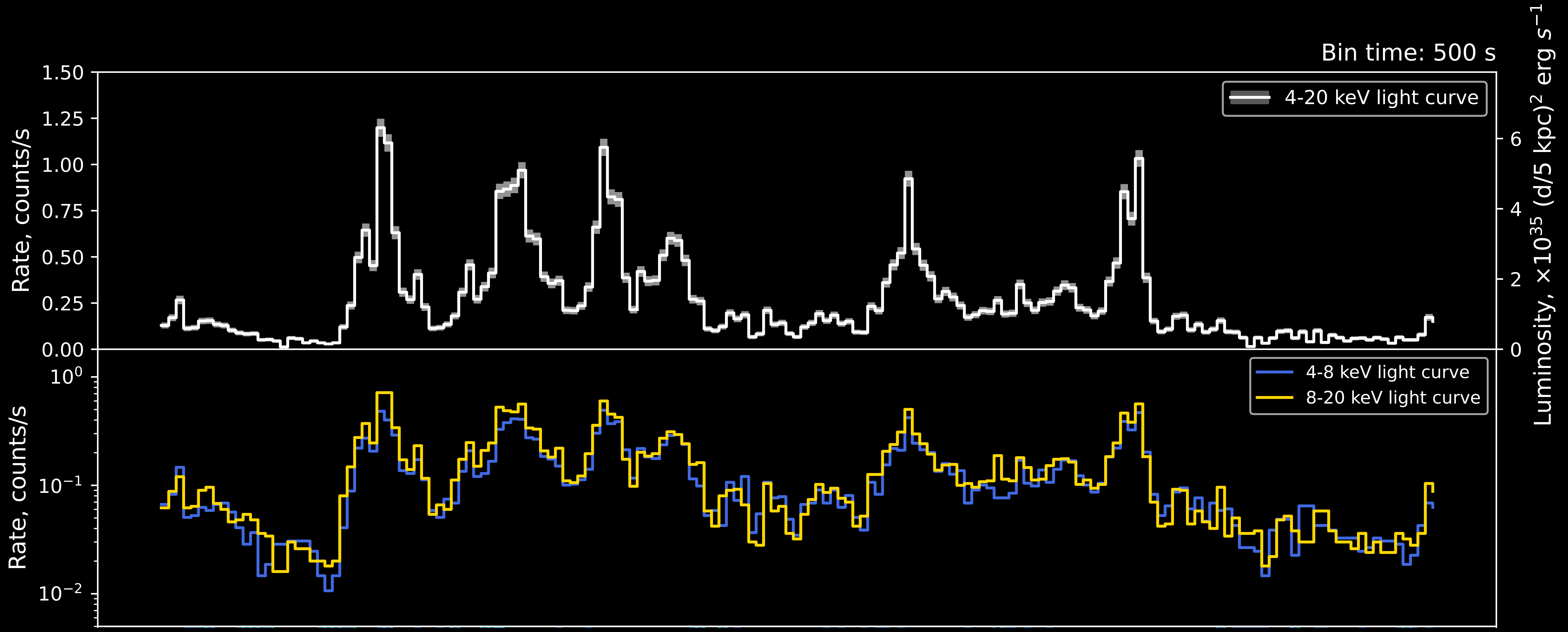

Bin time: 500 s
4-20 keV light curve
4-8 keV light curve
8-20 keV light curve
Rate, counts/s
Rate, counts/s
Luminosity, ×10^35 (d/5 kpc)^2 erg s^−1
1.50
1.25
1.00
0.75
0.50
0.25
0.00
10^0
10^−1
10^−2
6
4
2
0

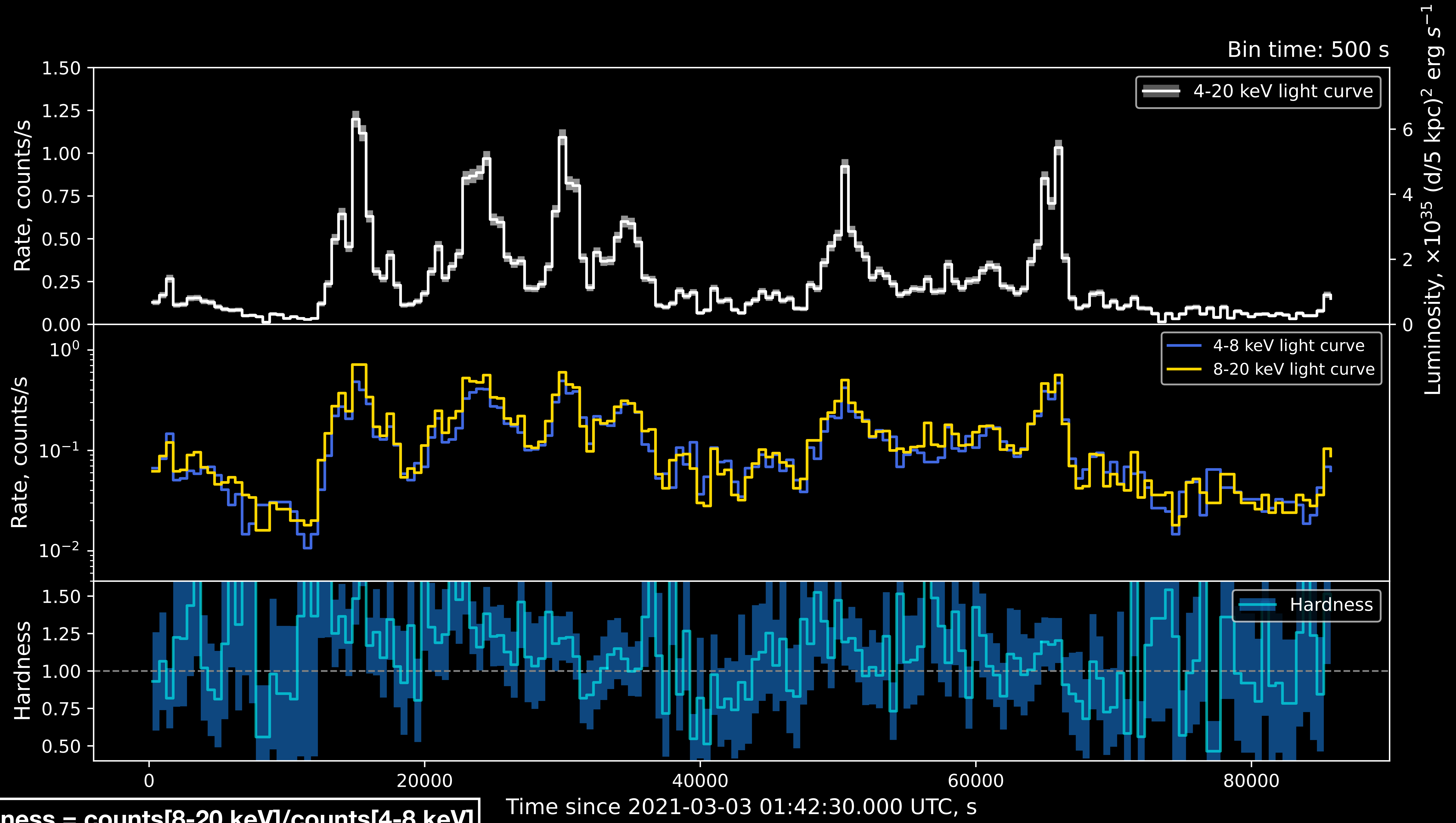

Hardness = counts[8-20 keV]/counts[4-8 keV]

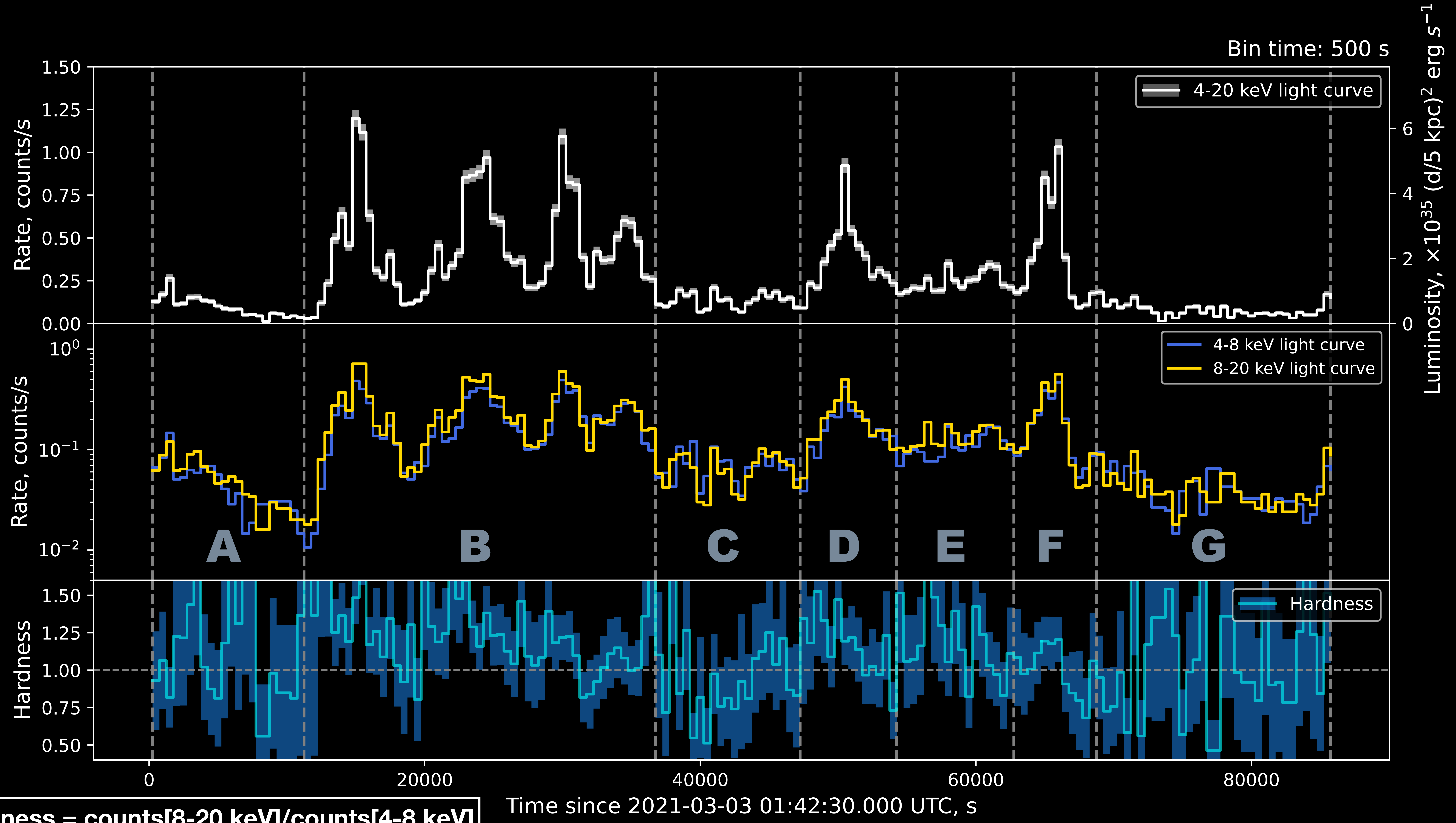

Hardness = counts[8-20 keV]/counts[4-8 keV]

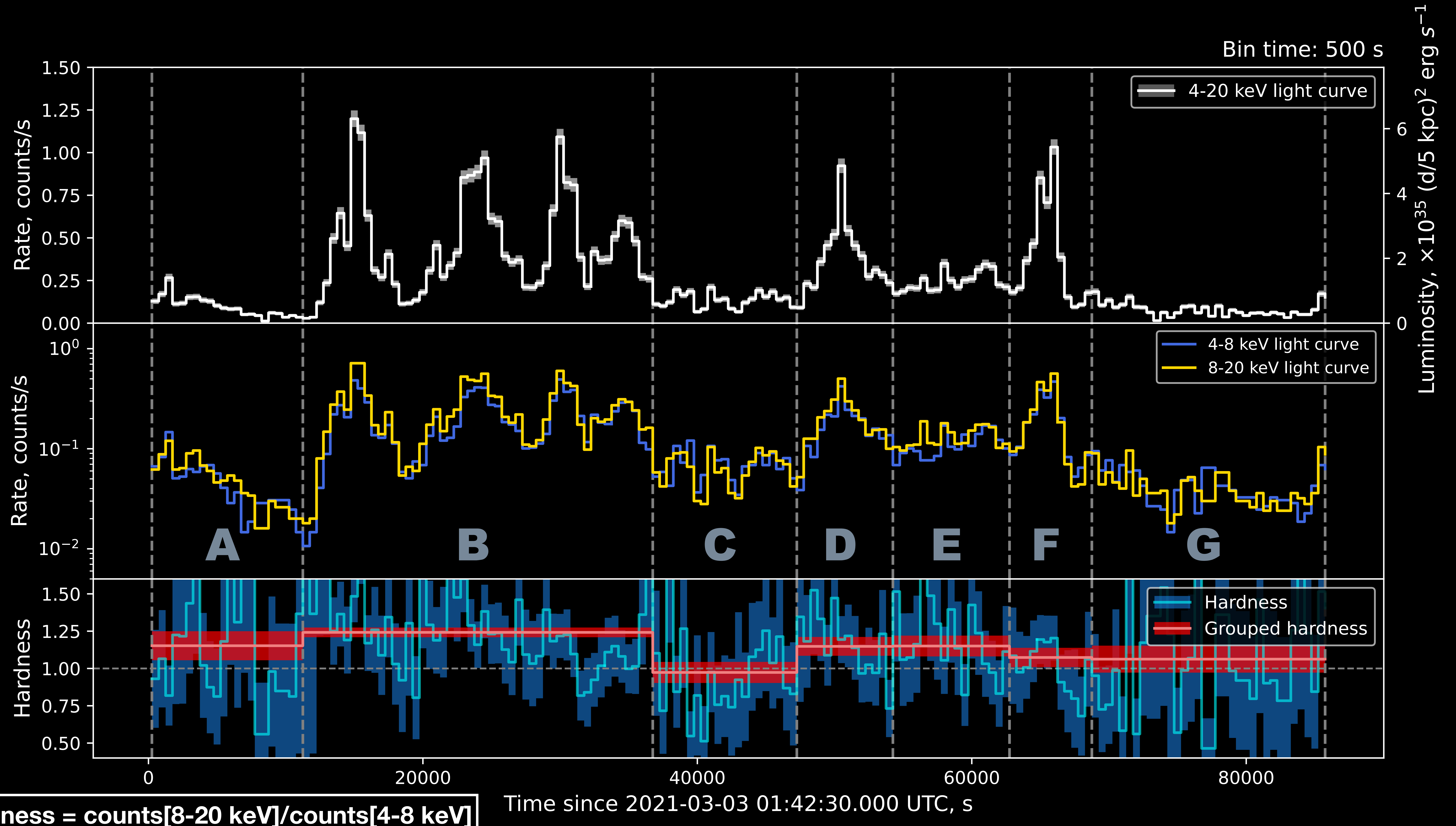

Hardness = counts[8-20 keV]/counts[4-8 keV]

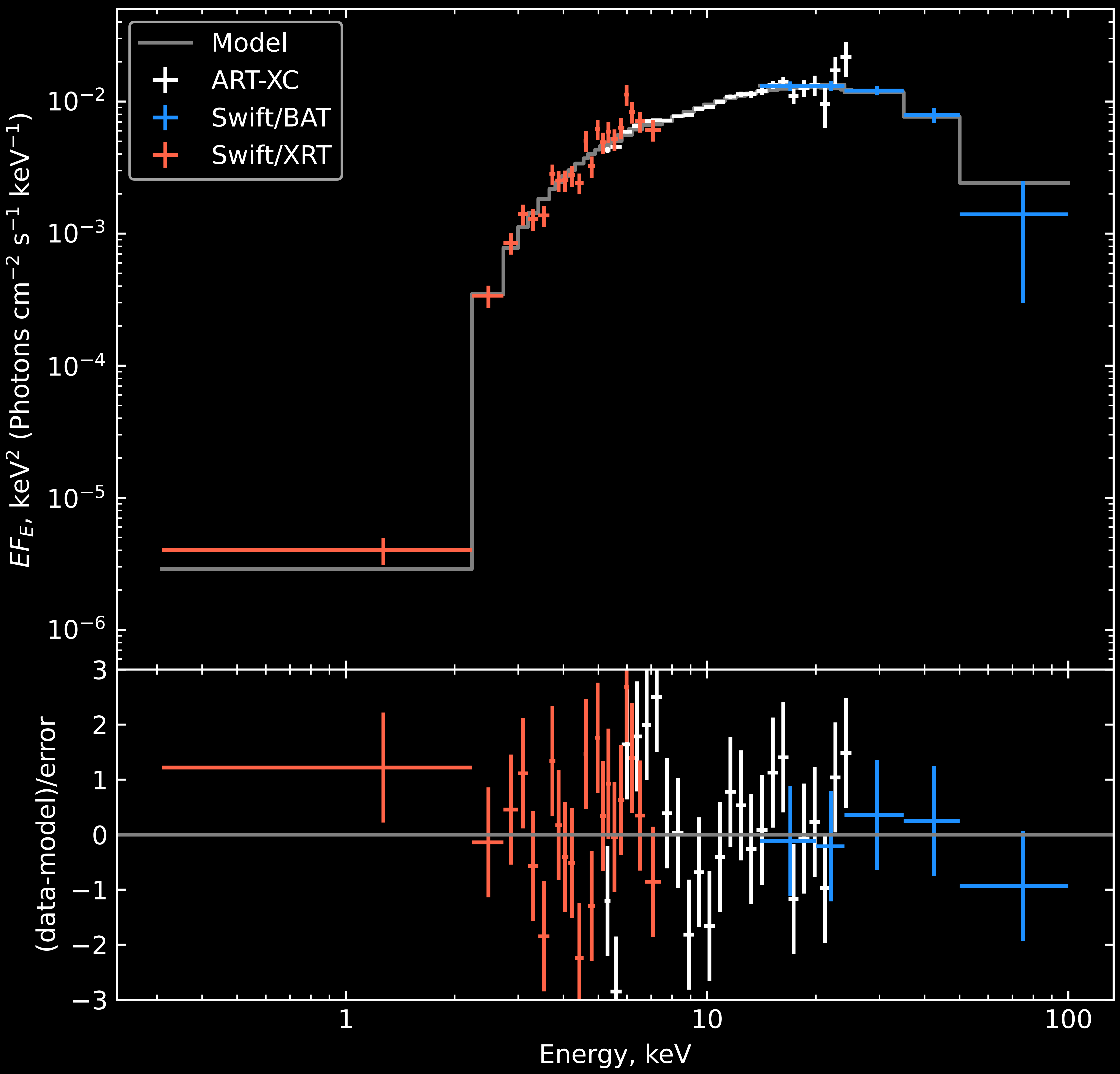

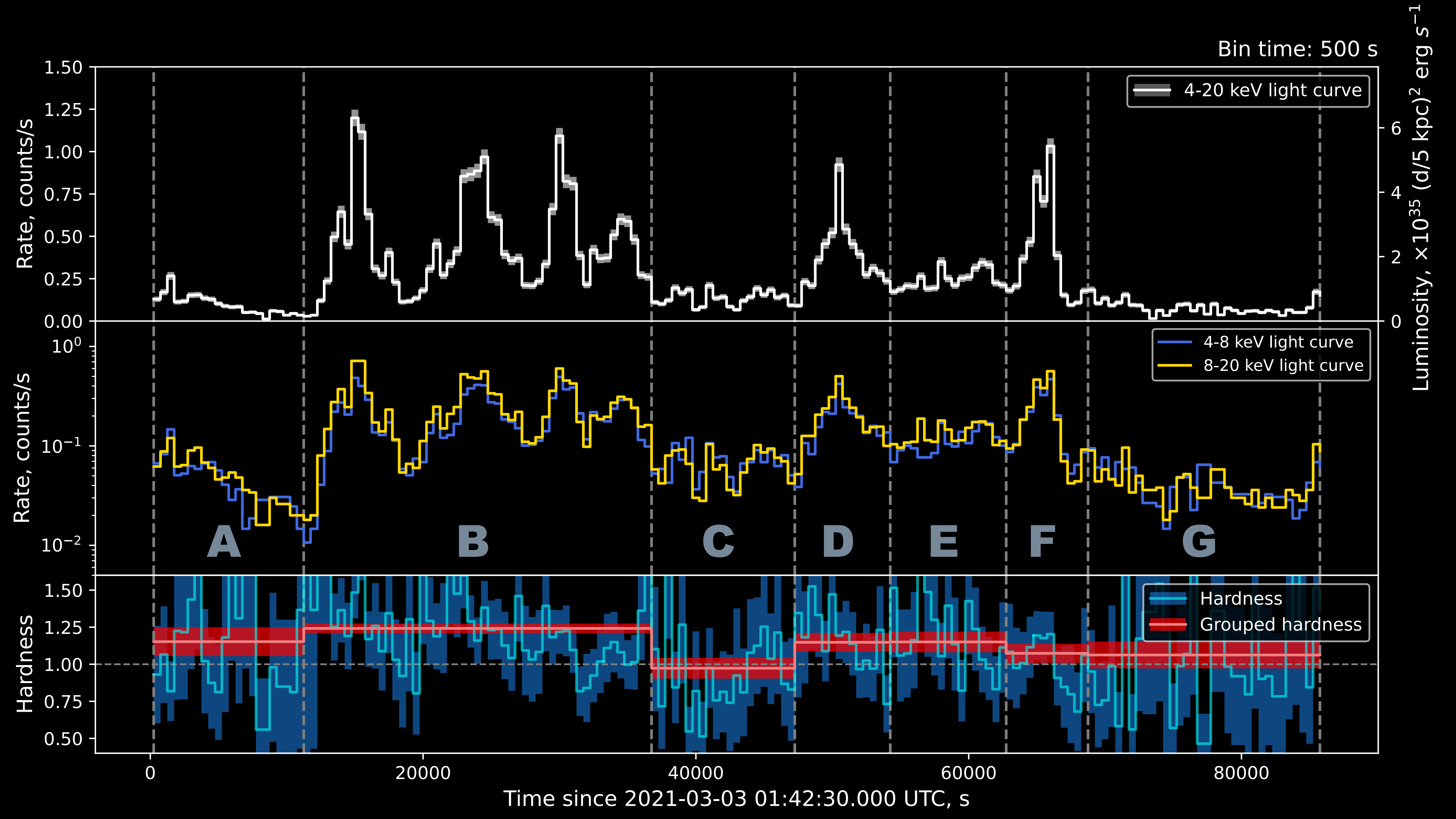

tbabs*cutoffpl

Segment	N_H, cm^{-2}	Γ	E_{cut}, keV
Full ART-XC + XRT + BAT	$(12 \pm 2) \times 10^{22}$	0.56 ± 0.15	13 ± 2
Full ART-XC	$(16 \pm 8) \times 10^{22}$	0.87 ± 0.35	15^{+13}_{-5}
Full ART-XC (fixed N_H)	12×10^{22}	0.67 ± 0.27	15^{+12}_{-5}
ART-XC: ACG (fixed N_H)	12×10^{22}	$0.58^{+0.84}_{-0.97}$	10^{+88}_{-5}
ART-XC: BDF (fixed N_H)	12×10^{22}	0.59 ± 0.27	15^{+9}_{-5}

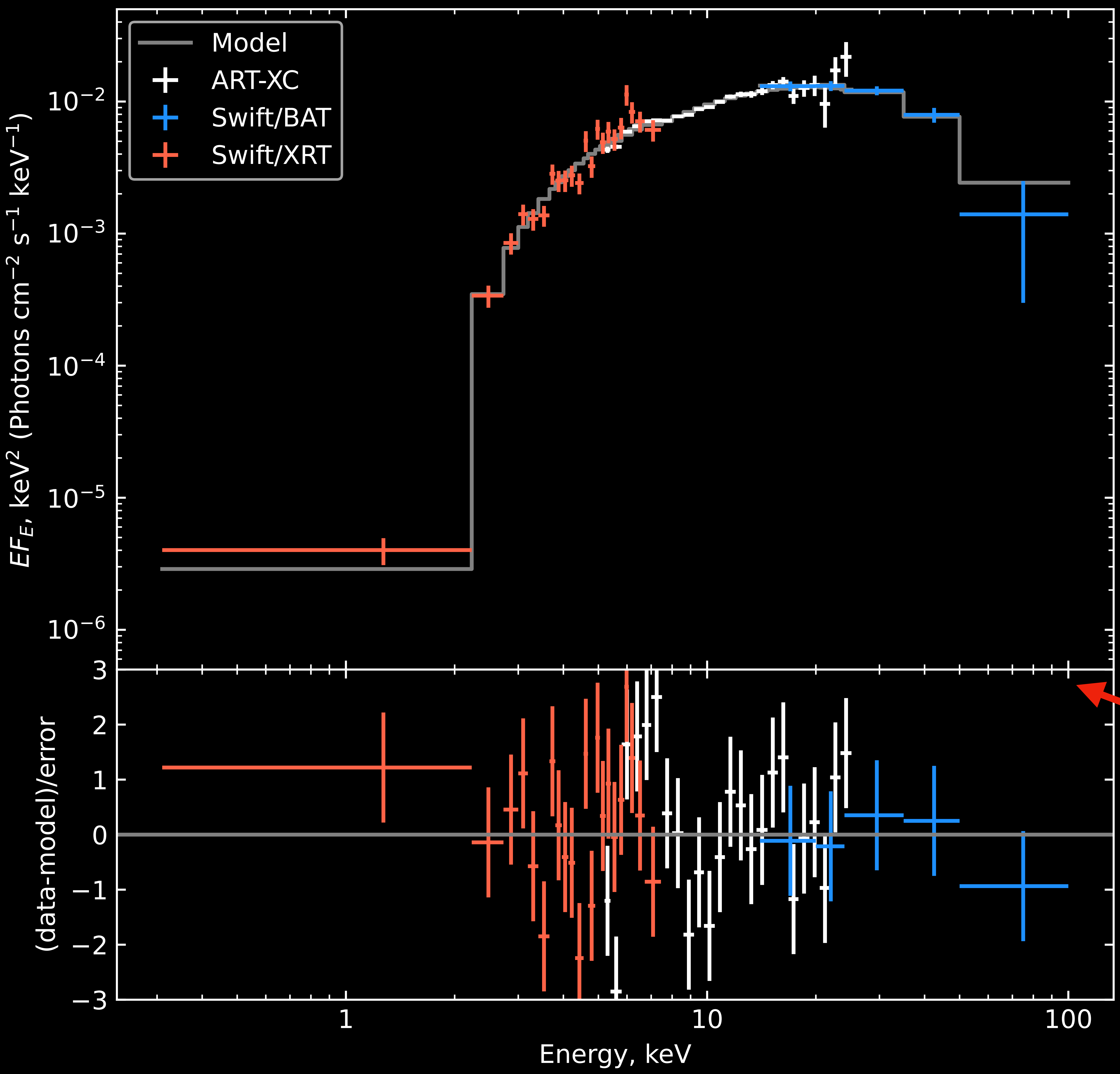

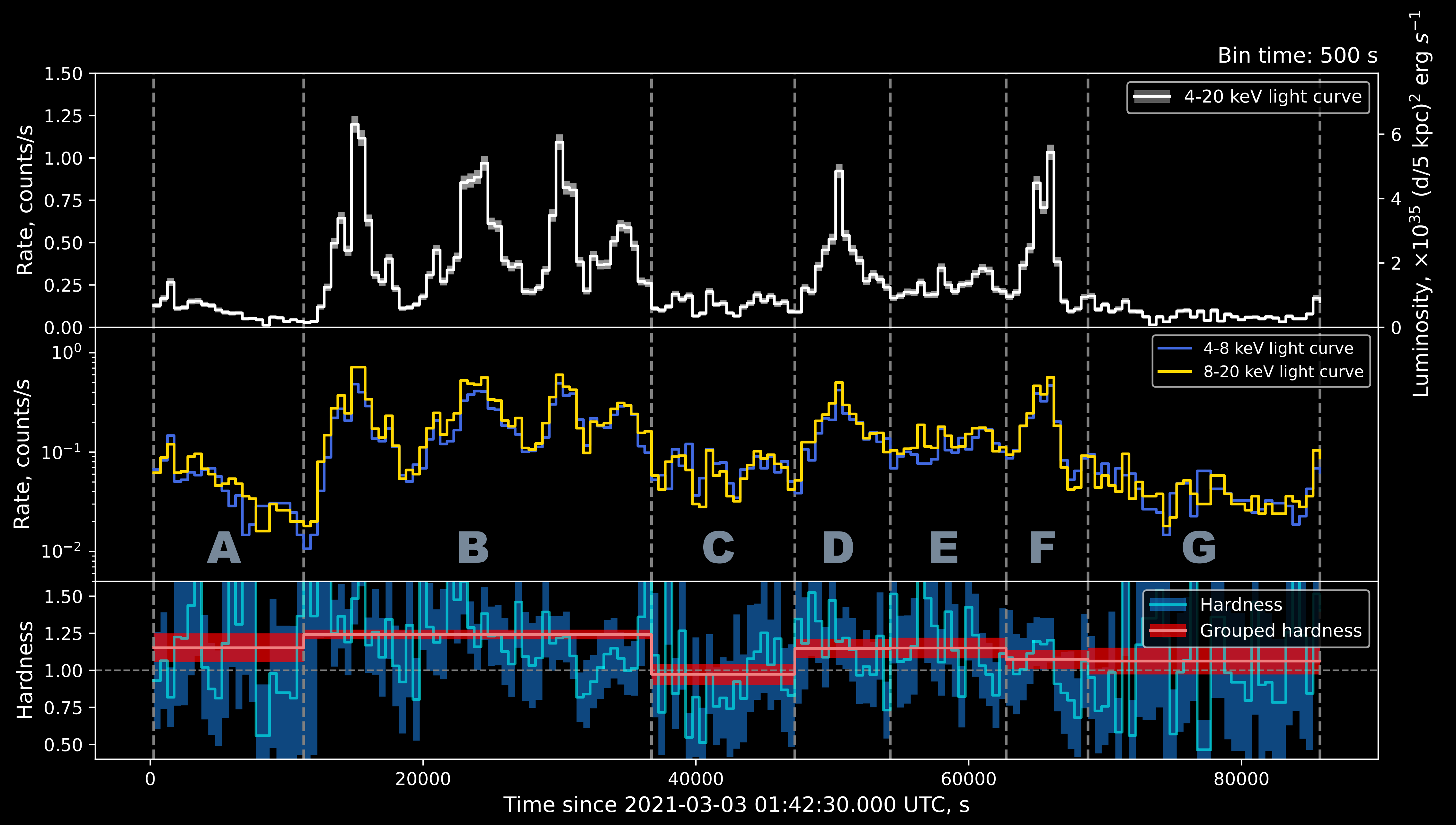

tbabs*cutoffpl

Segment	N_H, cm^{-2}	Γ	E_{cut}, keV
Full ART-XC + XRT + BAT	$(12 \pm 2) \times 10^{22}$	0.56 ± 0.15	13 ± 2
Full ART-XC	$(16 \pm 8) \times 10^{22}$	0.87 ± 0.35	15^{+13}_{-5}
Full ART-XC (fixed N_H)	12×10^{22}	0.67 ± 0.27	15^{+12}_{-5}
ART-XC: ACG (fixed N_H)	12×10^{22}	$0.58^{+0.84}_{-0.97}$	10^{+88}_{-5}
ART-XC: BDF (fixed N_H)	12×10^{22}	0.59 ± 0.27	15^{+9}_{-5}

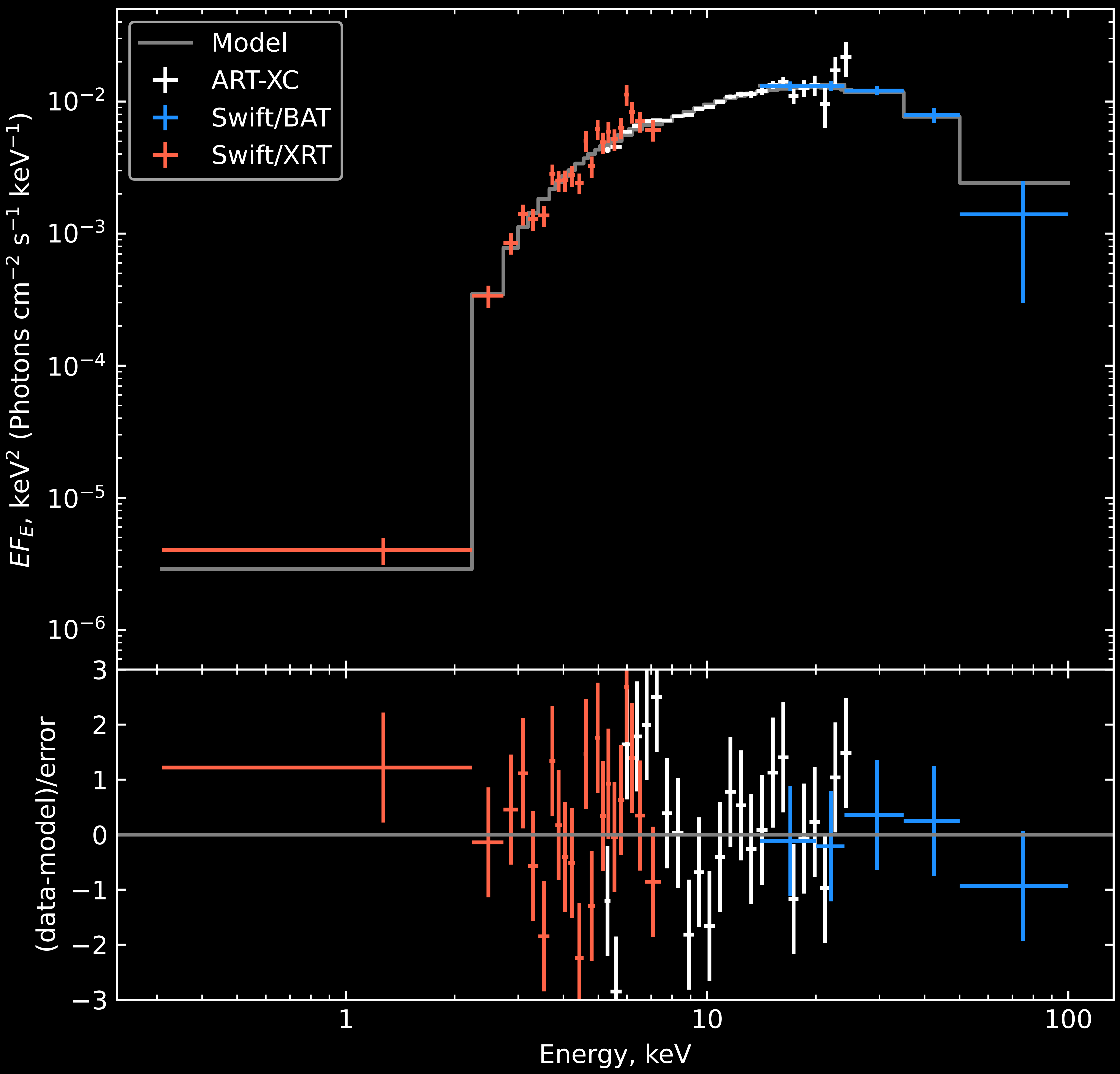

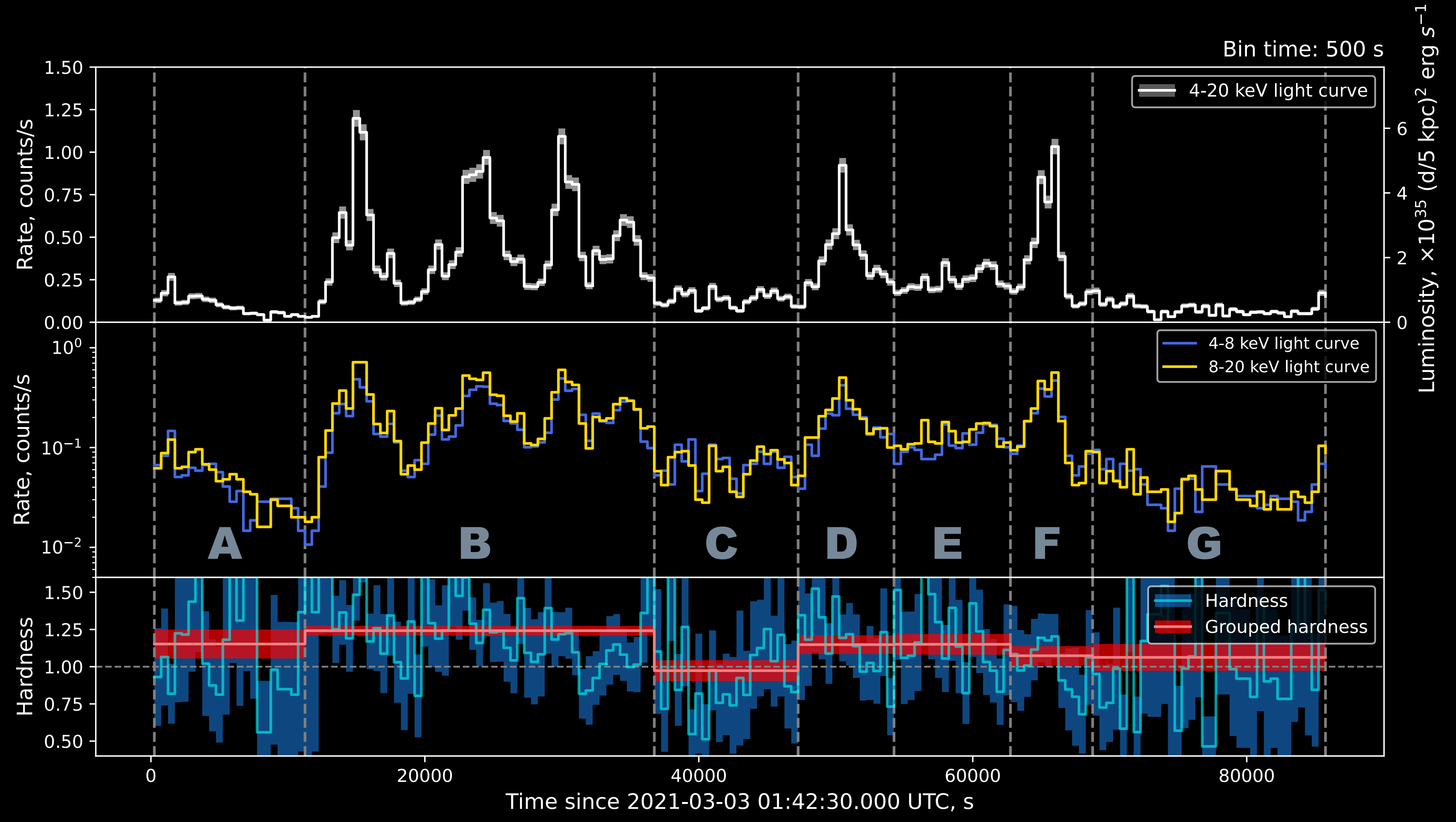

tbabs*cutoffpl

Segment	N_H, cm^{-2}	Γ	E_{cut}, keV
Full ART-XC + XRT + BAT	$(12 \pm 2) \times 10^{22}$	0.56 ± 0.15	13 ± 2
Full ART-XC	$(16 \pm 8) \times 10^{22}$	0.87 ± 0.35	15^{+13}_{-5}
Full ART-XC (fixed N_H)	12×10^{22}	0.67 ± 0.27	15^{+12}_{-5}
ART-XC: ACG (fixed N_H)	12×10^{22}	$0.58^{+0.84}_{-0.97}$	10^{+88}_{-5}
ART-XC: BDF (fixed N_H)	12×10^{22}	0.59 ± 0.27	15^{+9}_{-5}

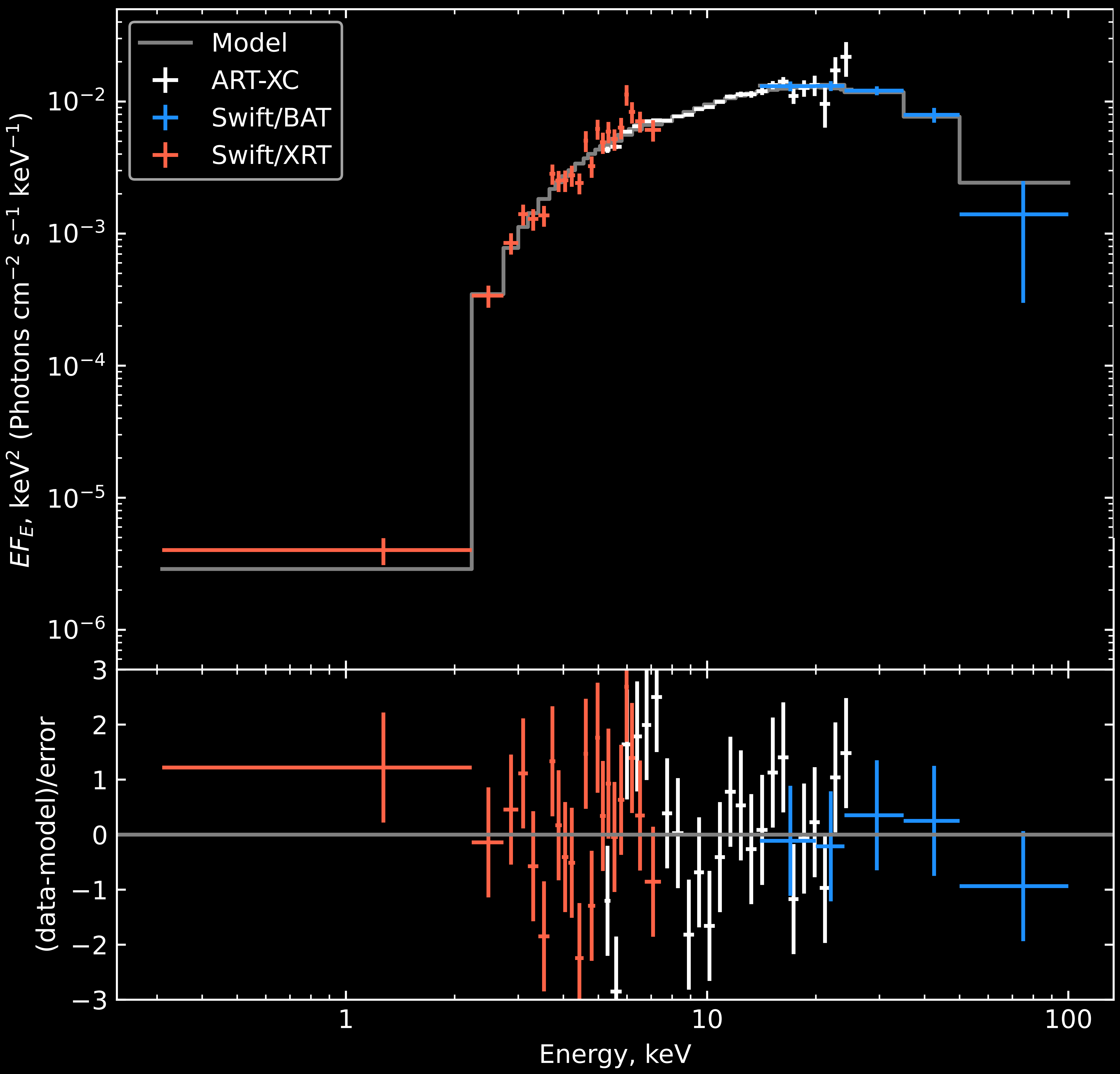

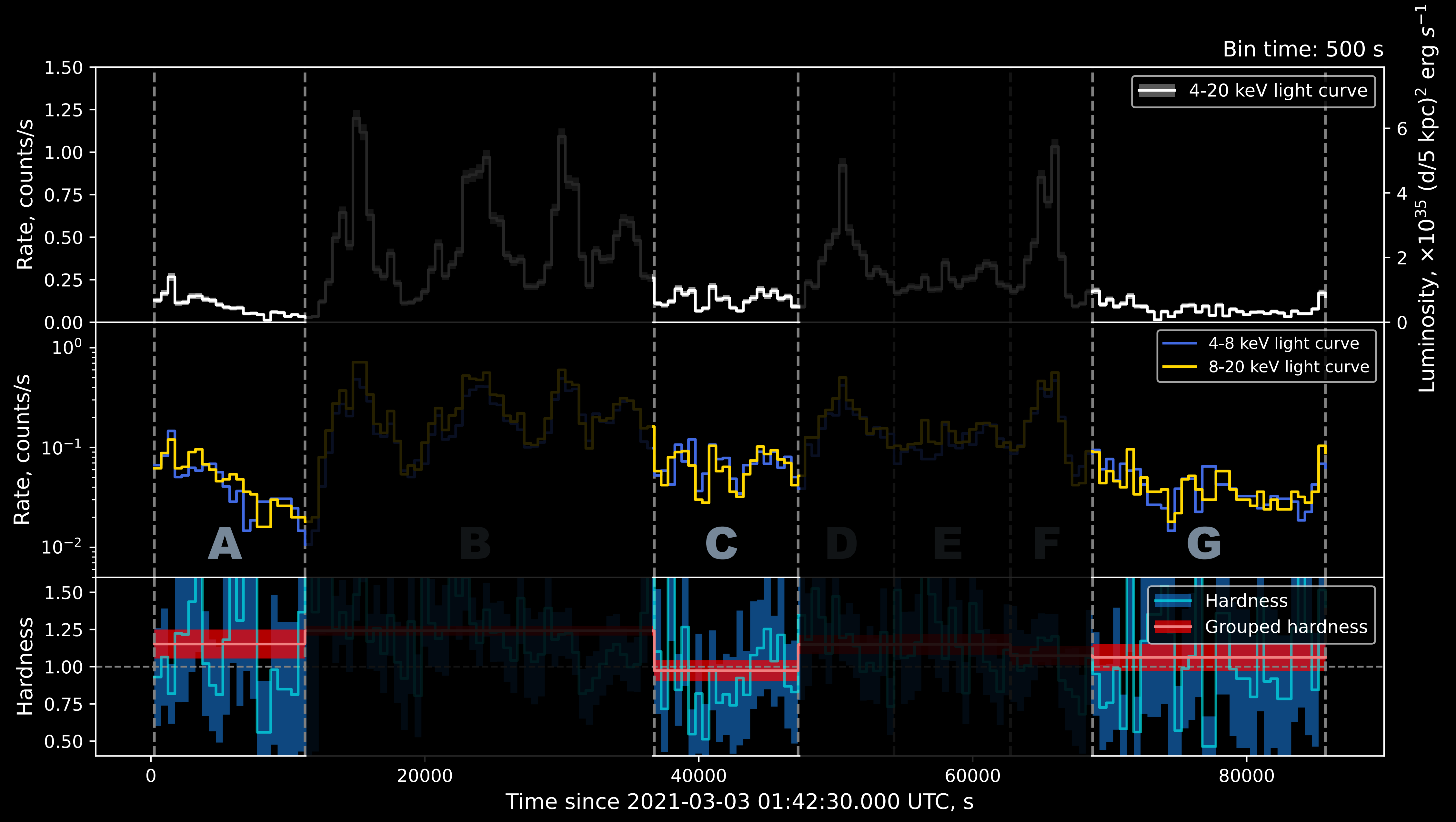

tbabs*cutoffpl

Segment	N_H, cm^{-2}	Γ	E_{cut}, keV
Full ART-XC + XRT + BAT	$(12 \pm 2) \times 10^{22}$	0.56 ± 0.15	13 ± 2
Full ART-XC	$(16 \pm 8) \times 10^{22}$	0.87 ± 0.35	15^{+13}_{-5}
Full ART-XC (fixed N_H)	12×10^{22}	0.67 ± 0.27	15^{+12}_{-5}
ART-XC: ACG (fixed N_H)	12×10^{22}	$0.58^{+0.84}_{-0.97}$	10^{+88}_{-5}
ART-XC: BDF (fixed N_H)	12×10^{22}	0.59 ± 0.27	15^{+9}_{-5}

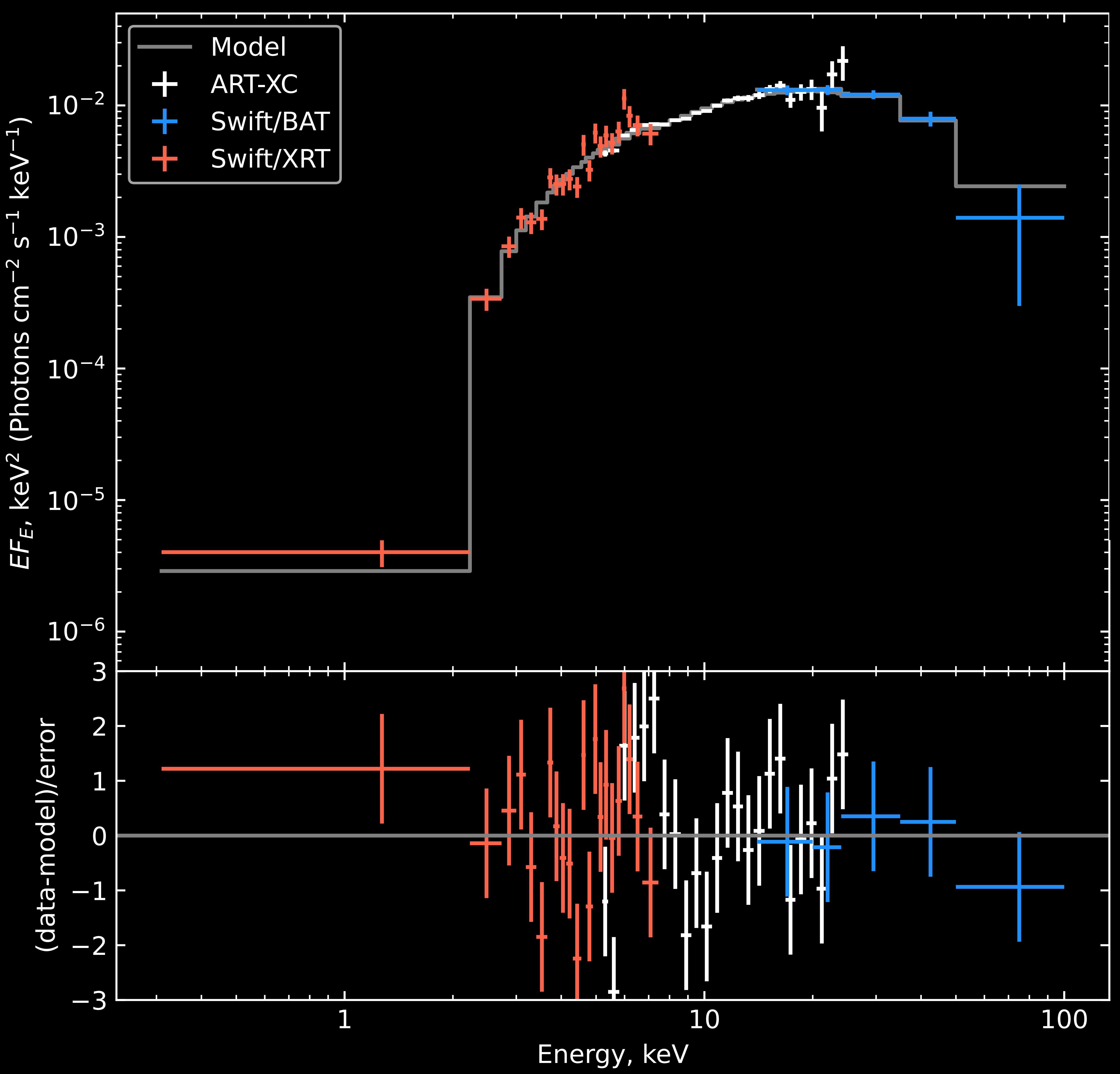

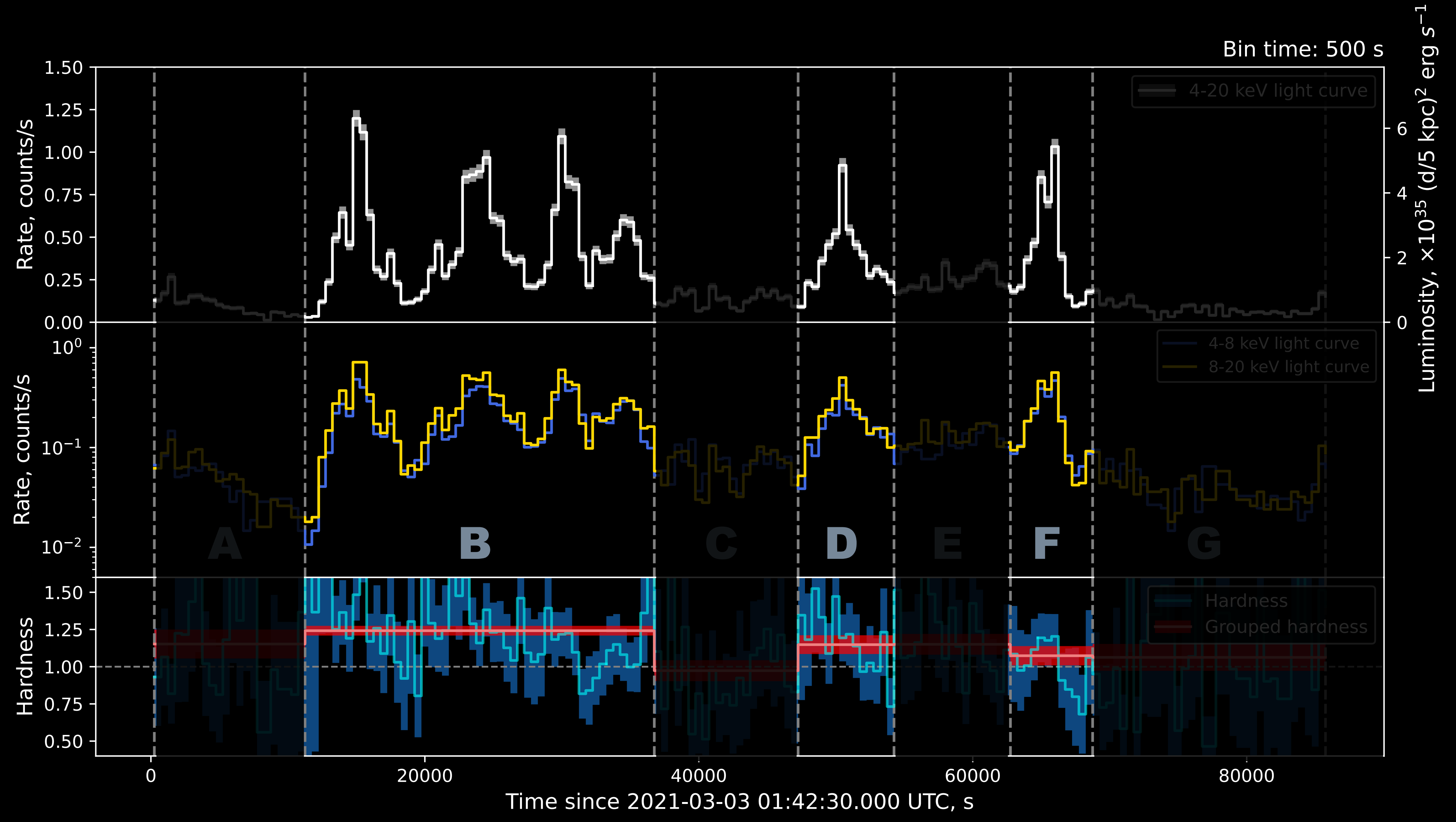

tbabs*cutoffpl

Segment	N_H, cm^{-2}	Γ	E_{cut}, keV
Full ART-XC + XRT + BAT	$(12 \pm 2) \times 10^{22}$	0.56 ± 0.15	13 ± 2
Full ART-XC	$(16 \pm 8) \times 10^{22}$	0.87 ± 0.35	15^{+13}_{-5}
Full ART-XC (fixed N_H)	12×10^{22}	0.67 ± 0.27	15^{+12}_{-5}
ART-XC: ACG (fixed N_H)	12×10^{22}	$0.58^{+0.84}_{-0.97}$	10^{+88}_{-5}
ART-XC: BDF (fixed N_H)	12×10^{22}	0.59 ± 0.27	15^{+9}_{-5}

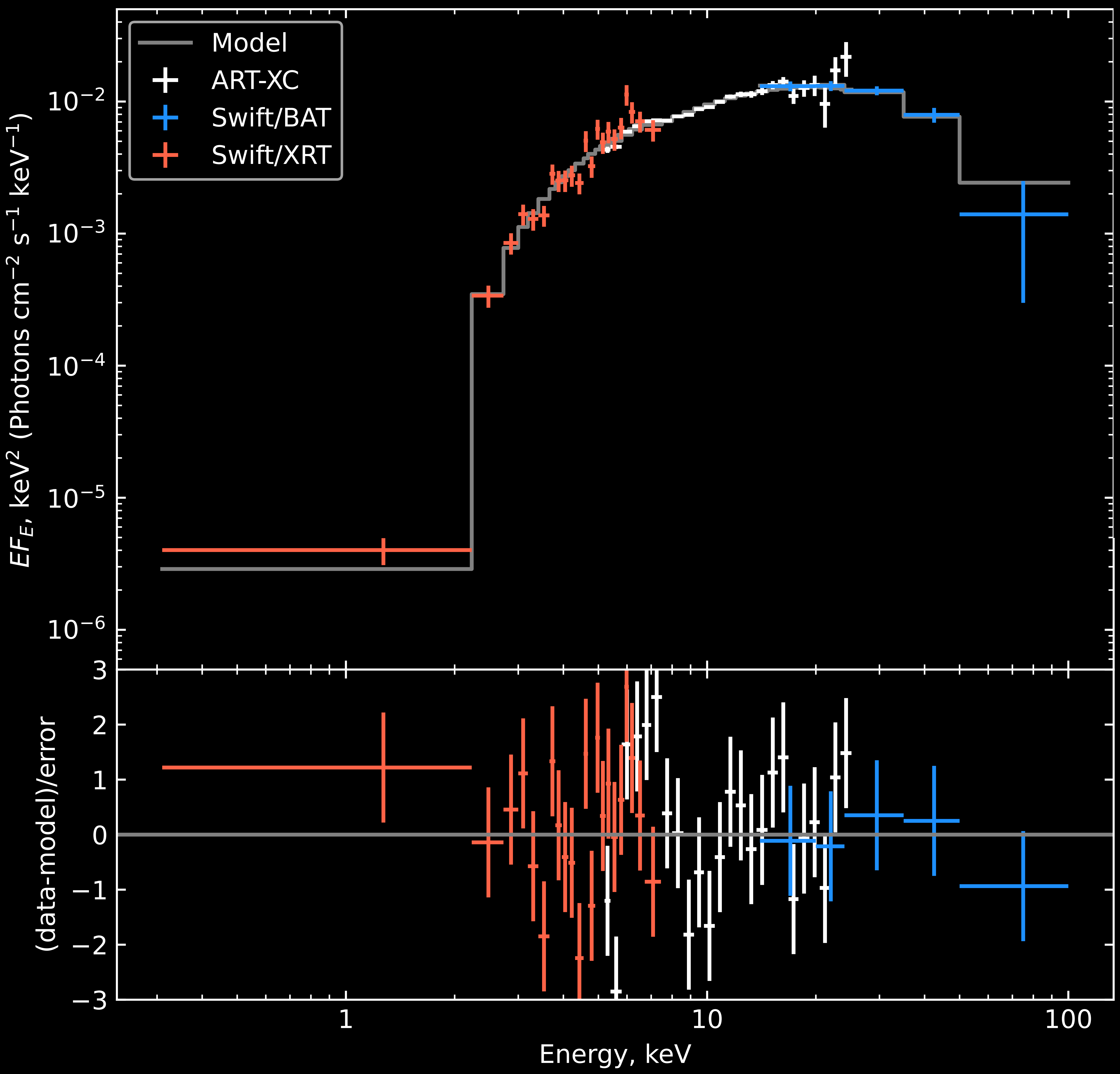

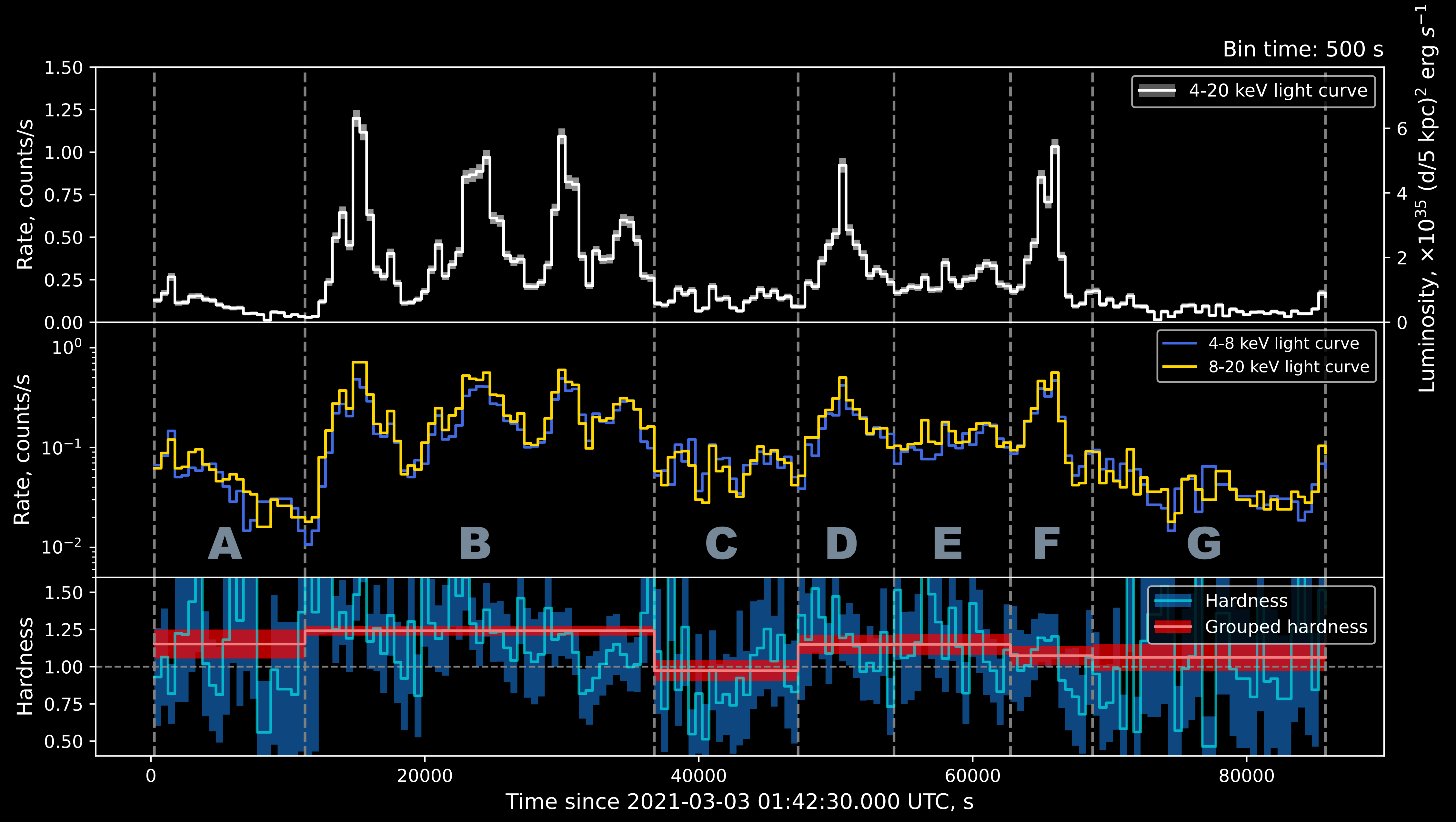

tbabs*cutoffpl

Segment	N_H, cm^{-2}	Γ	E_{cut}, keV
Full ART-XC + XRT + BAT	$(12 \pm 2) \times 10^{22}$	0.56 ± 0.15	13 ± 2
Full ART-XC	$(16 \pm 8) \times 10^{22}$	0.87 ± 0.35	15^{+13}_{-5}
Full ART-XC (fixed N_H)	12×10^{22}	0.67 ± 0.27	15^{+12}_{-5}
ART-XC: ACG (fixed N_H)	12×10^{22}	$0.58^{+0.84}_{-0.97}$	10^{+88}_{-5}
ART-XC: BDF (fixed N_H)	12×10^{22}	0.59 ± 0.27	15^{+9}_{-5}

"Colorless" variability

$$L_{bol} = (1.38 \pm 0.05) \times 10^{35} (\mathrm{d}/5\ \mathrm{kpc})^2\ \mathrm{erg\ s}^{-1} < L_{crit} = 4 \times 10^{36}\ \mathrm{erg\ s}^{-1}$$

Settling accretion?

$L_{crit} = 4 \times 10^{36}$ erg s^{-1} $(\dot{M}_{crit} = 4 \times 10^{16}$ g s$^{-1})$ Shakura et al., 2012

Quasi-spherical subsonic settling accretion:

$\dot{M} < \dot{M}_{crit} = 4 \times 10^{16}$ g s^{-1}

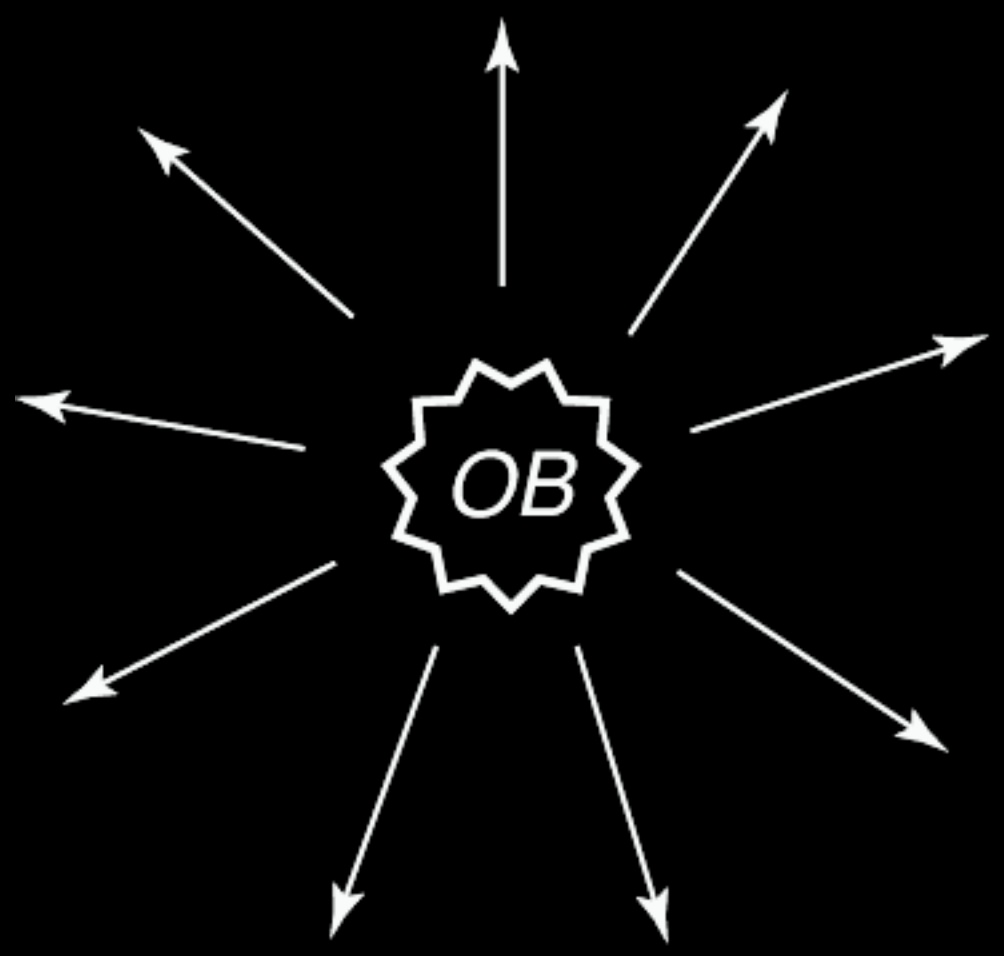

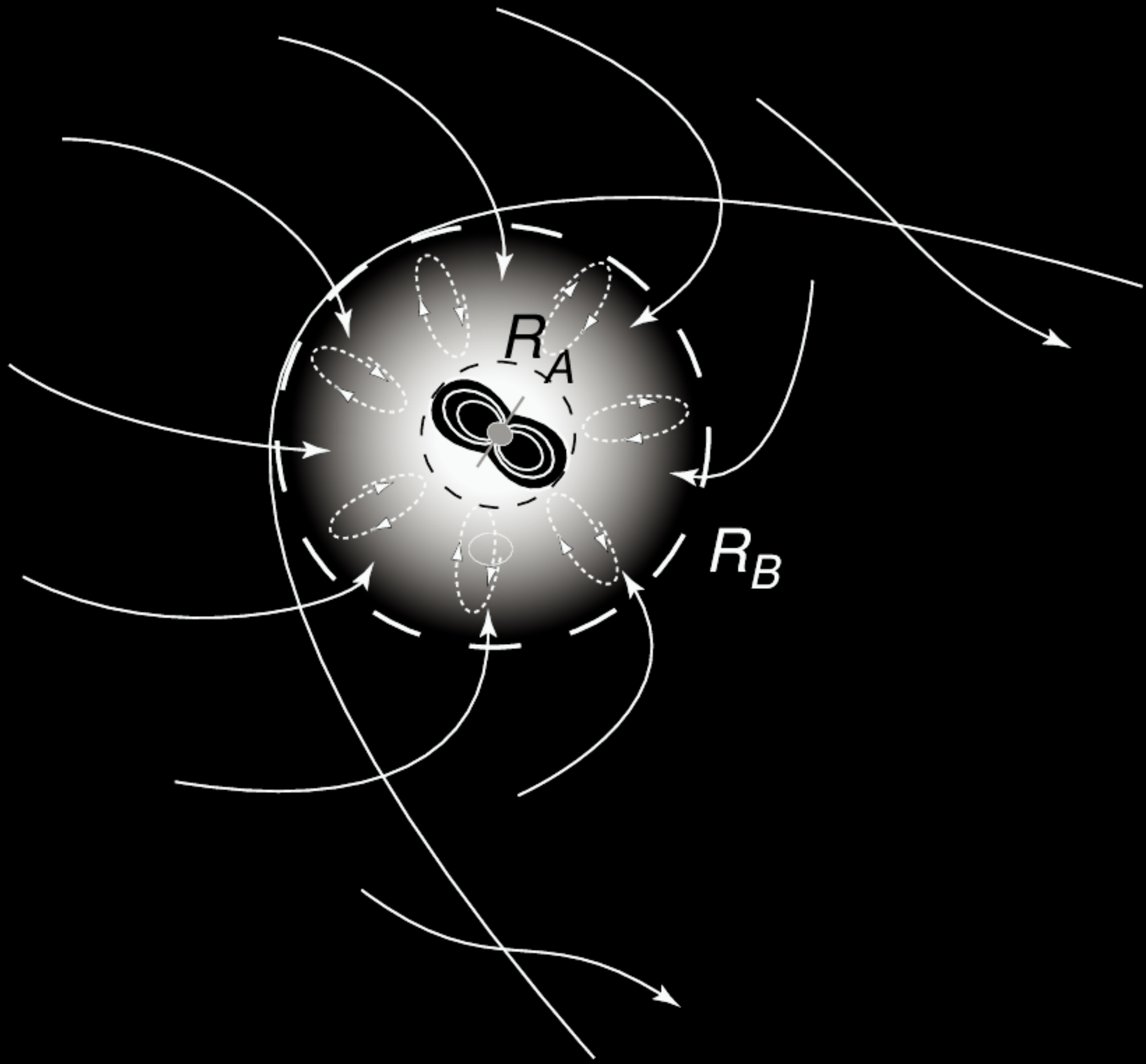

Bondi-Hoyle-Littleton accretion (supersonic):

$\dot{M} > \dot{M}_{crit} = 4 \times 10^{16}$ g s^{-1}

Bondi, 1952

Sidoli et al. 2019, Shakura et al. 2014

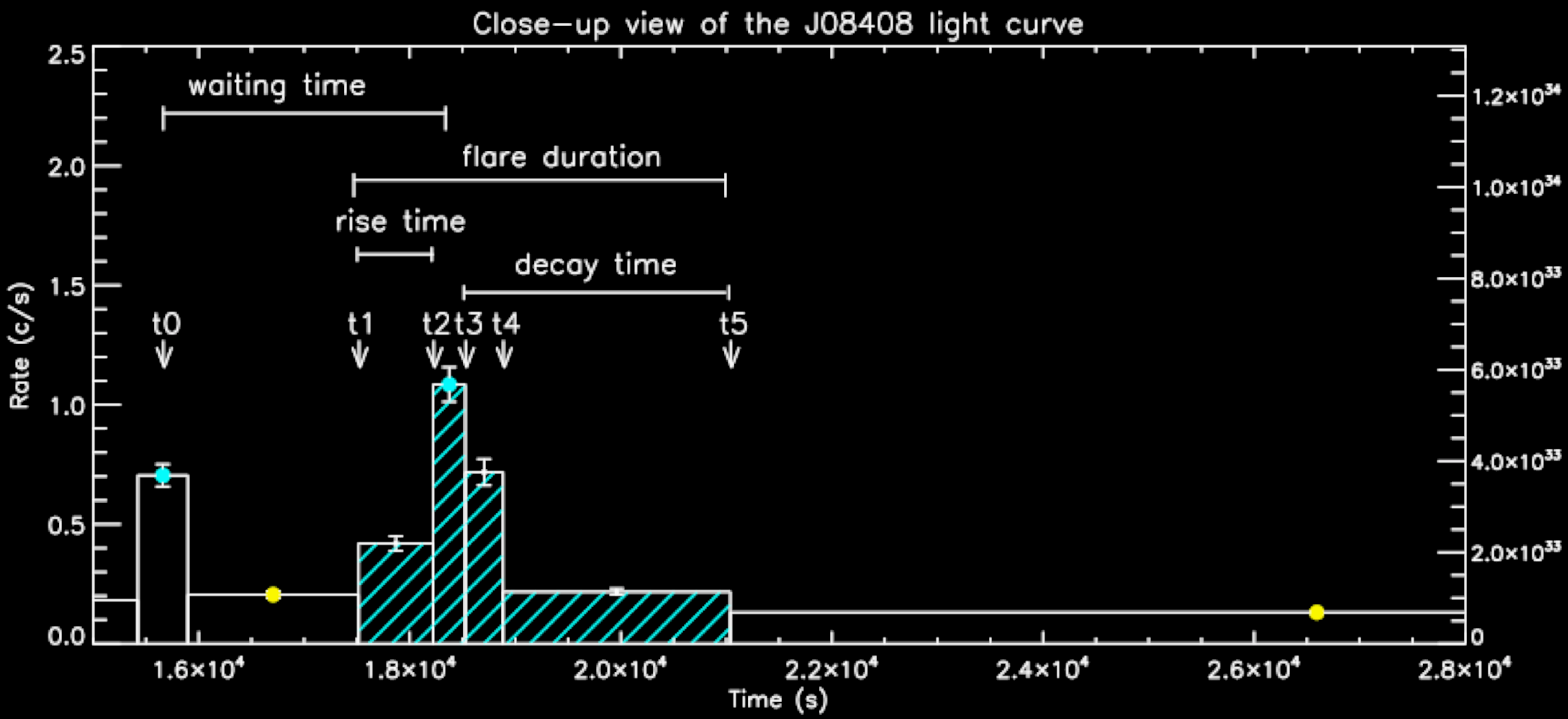

Waiting time $\Delta T \sim 130[\mathrm{s}]\dot{M}_{16}^{-1}$

$\Delta E \sim 3 \times 10^{35}[\text{erg s}^{-1}]v_8^3 \Delta t$

$\delta t_{rise} \sim 30[\mathrm{s}]\dot{M}_{16}^{-2/3}$

$$\frac{\Delta E}{\Delta T} = 10^{36}[\text{erg s}^{-1}]\dot{M}_{16}$$

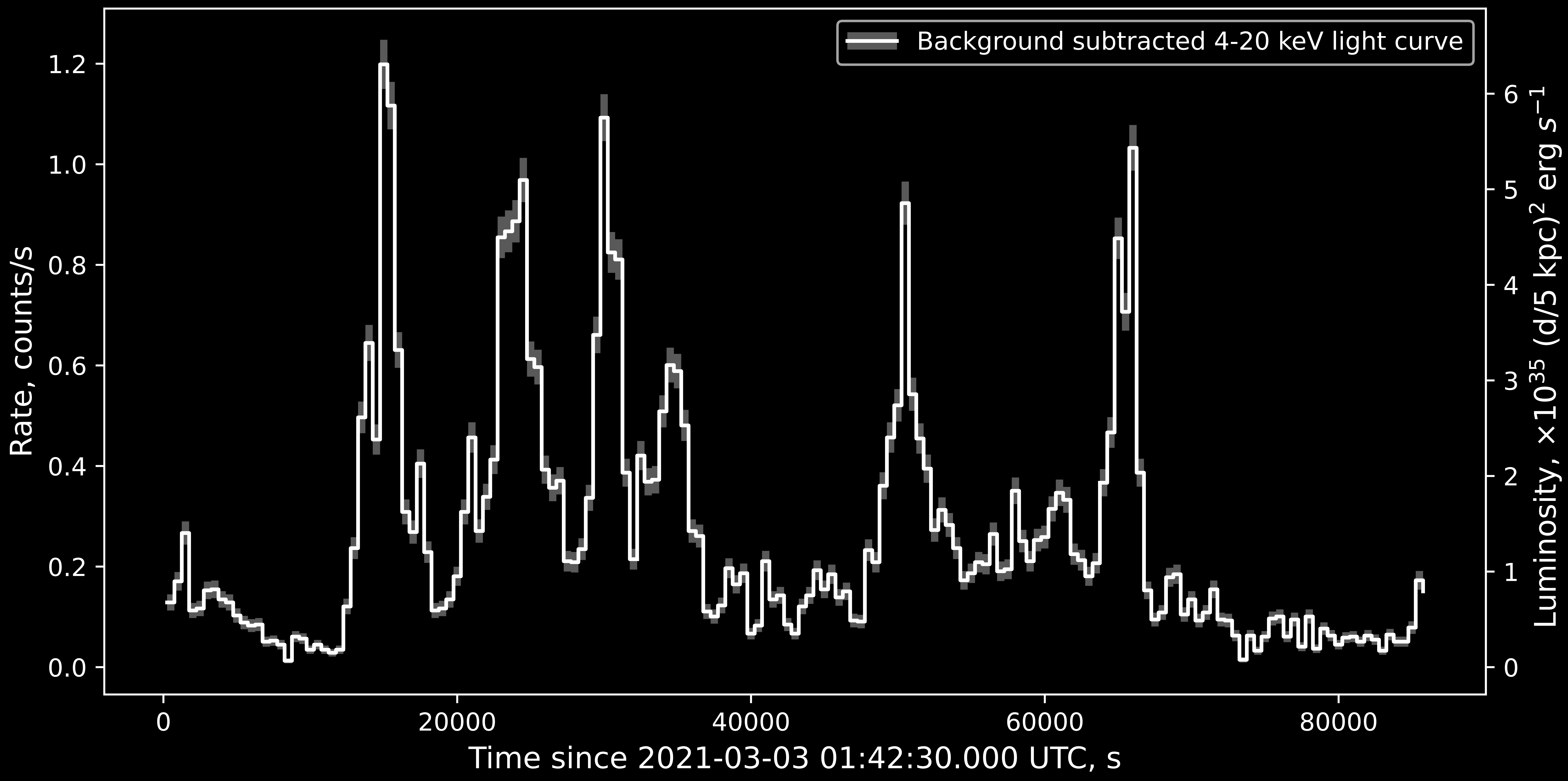

Background subtracted 4-20 keV light curve
Rate, counts/s
Luminosity, $\times 10^{35}$ (d/5 kpc)^2 erg s^{-1}
Time since 2021-03-03 01:42:30.000 UTC, s
0.0
0.2
0.4
0.6
0.8
1.0
1.2
0
1
2
3
4
5
6
0
20000
40000
60000
80000

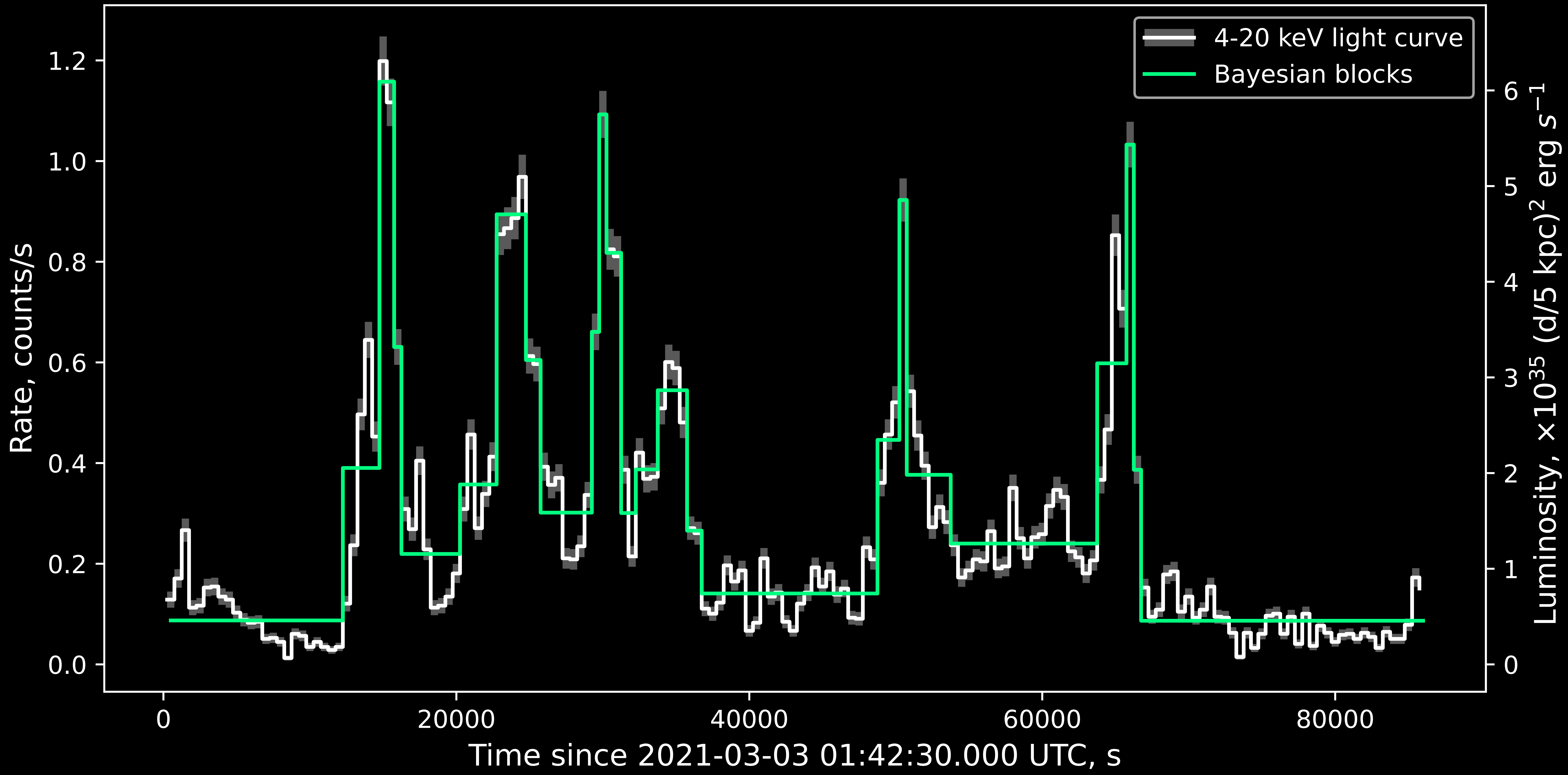

4-20 keV light curve
Bayesian blocks
Rate, counts/s
Luminosity, ×10^35 (d/5 kpc)^2 erg s^-1
Time since 2021-03-03 01:42:30.000 UTC, s
0.0
0.2
0.4
0.6
0.8
1.0
1.2
0
1
2
3
4
5
6
0
20000
40000
60000
80000

$v_w \approx 500$ km s^{-1} typical for HMXBs (Martinez-Nunez et al. 2017)

Rapid IR variability

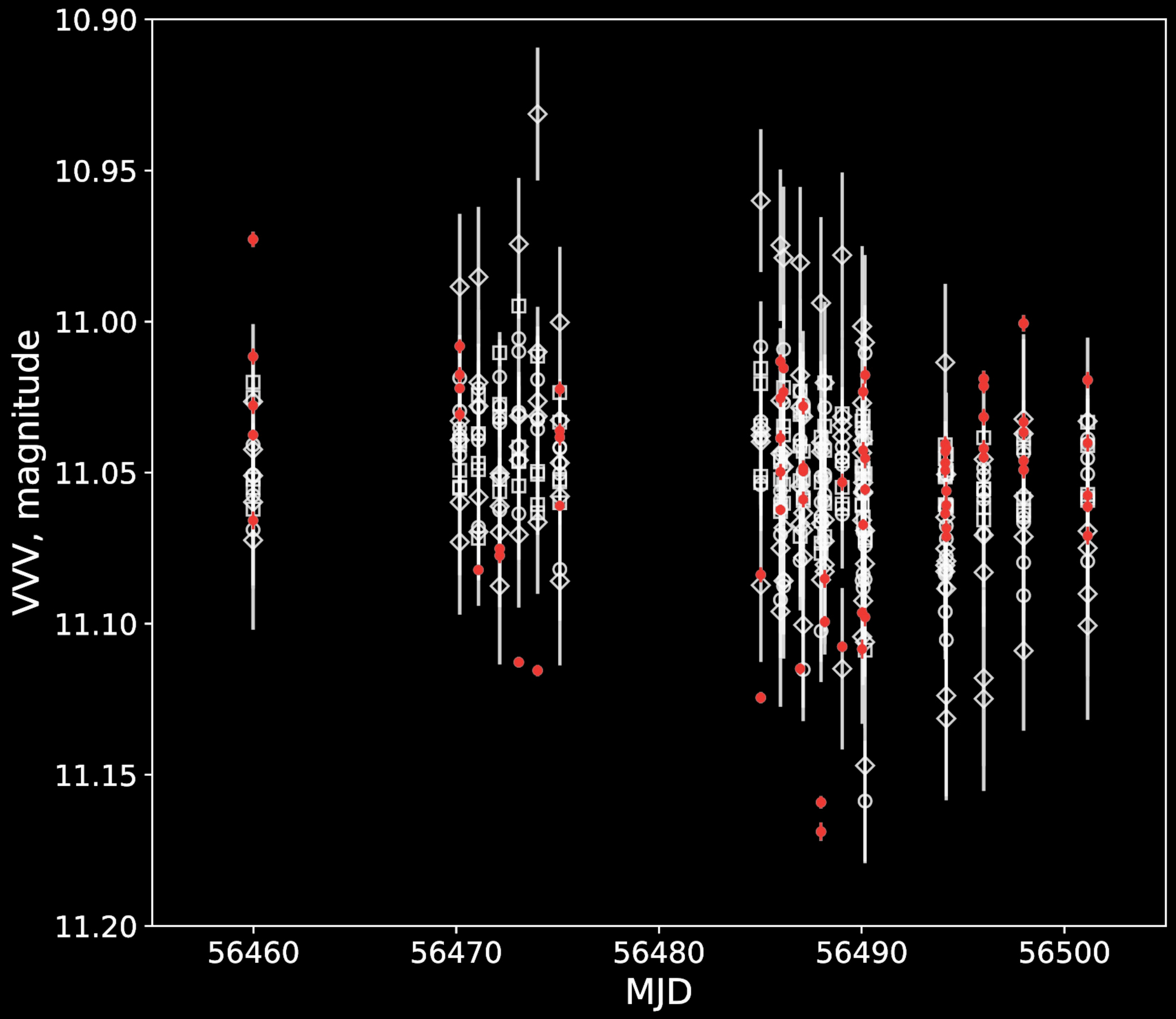

IGR J16195-4945 in Ks filter (red dots) according to the VVV survey. White markers show magnitudes of comparison stars normalized to the average magnitude of IGR J16195-4945

- **Changes in brightness for 0.1-0.2 magnitudes over several days**
- **Atypical for blue supergiants. Usual variability in range 0.02-0.04 (Buysschaert et al. 2015; Aerts et al. 2017)**

3A 1954+319

- Discovered by the *Uhuru* (Forman et al. 1978)
- Slowest NS in XBs (spin period ~5 hours; Corbert et al. 2008)

  with spin-ups and spin-downs (Marcu et al. 2011)
- SyXB with M4-5 III optical companion at a distance of 1.7 kpc (Masetti et al. 2006)

3A 1954+319

- Discovered by the *Uhuru* (Forman et al. 1978)
- Slowest NS in XBs (spin period ~5 hours; Corbert et al. 2008)

  with spin-ups and spin-downs (Marcu et al. 2011)
- ~~SyXB with M4-5 III optical companion at a distance of 1.7 kpc (Masetti et al. 2006)~~
- Gaia revealed that 3A 1954+319 is SgXB with RSG donor at a distance of ~3.3 kpc (Hinkle et al. 2020)
- NS may have magnetar-like magnetic field B $\gtrsim 10^{14}$ G or settling accretion regime (Enoto et al. 2014, Bozzo et al. 2022)

NuSTAR

3-79 keV

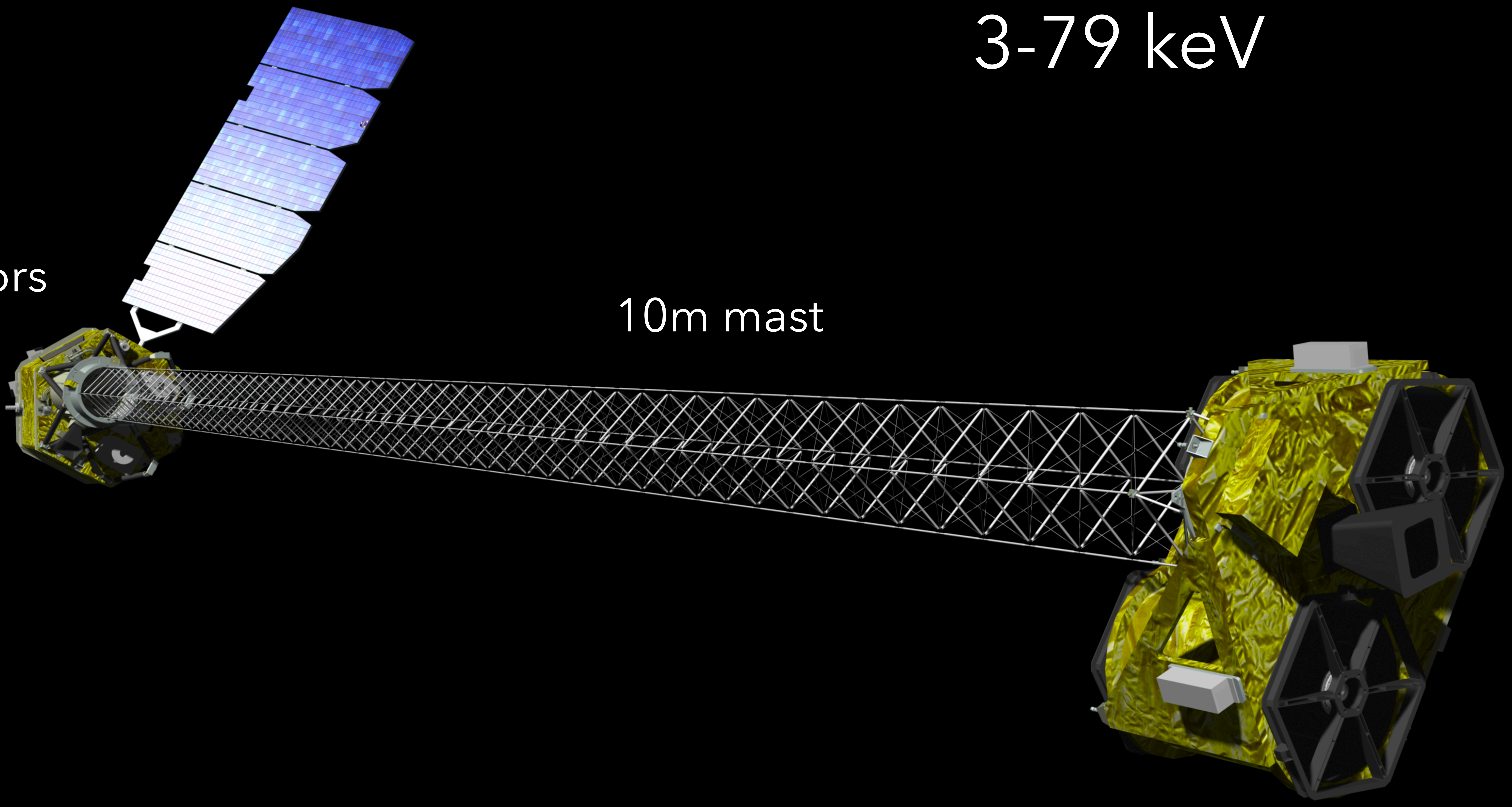

Harrison et al. 2013

NuSTAR

3-79 keV

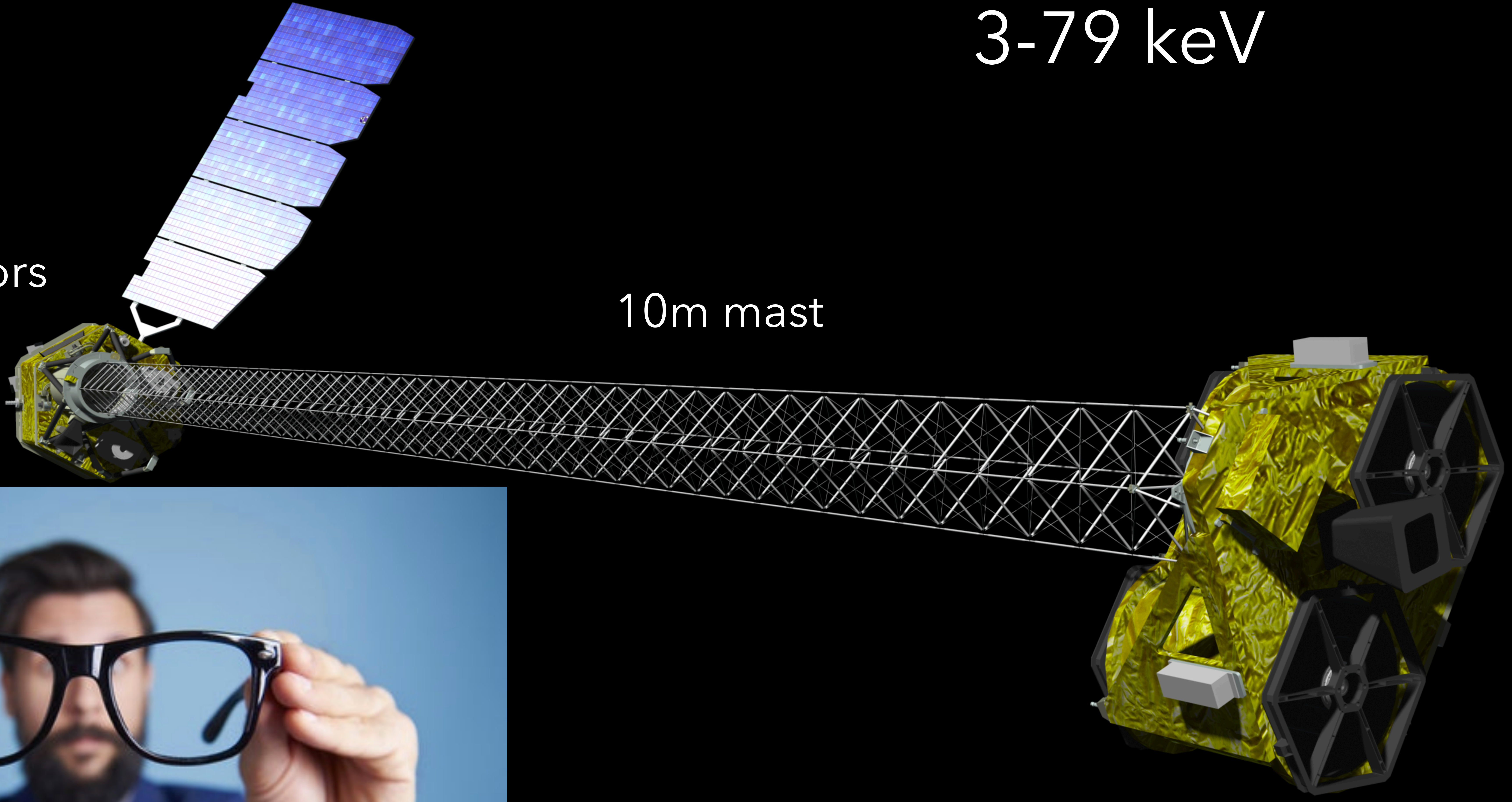

Harrison et al. 2013

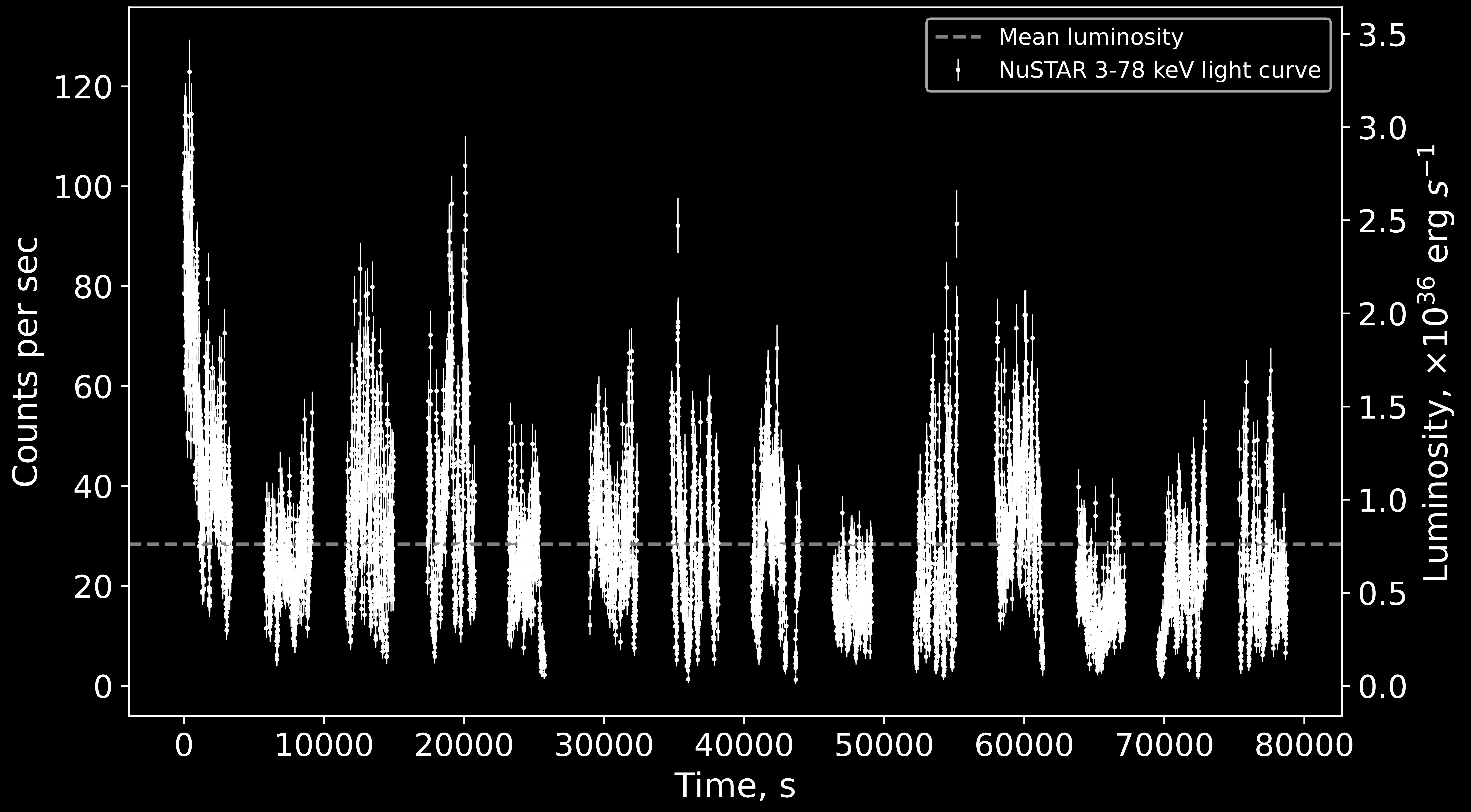

Mean luminosity
NuSTAR 3-78 keV light curve
Counts per sec
Luminosity, $\times 10^{36}$ erg s^{-1}
Time, s
0
20
40
60
80
100
120
0.0
0.5
1.0
1.5
2.0
2.5
3.0
3.5
0
10000
20000
30000
40000
50000
60000
70000
80000

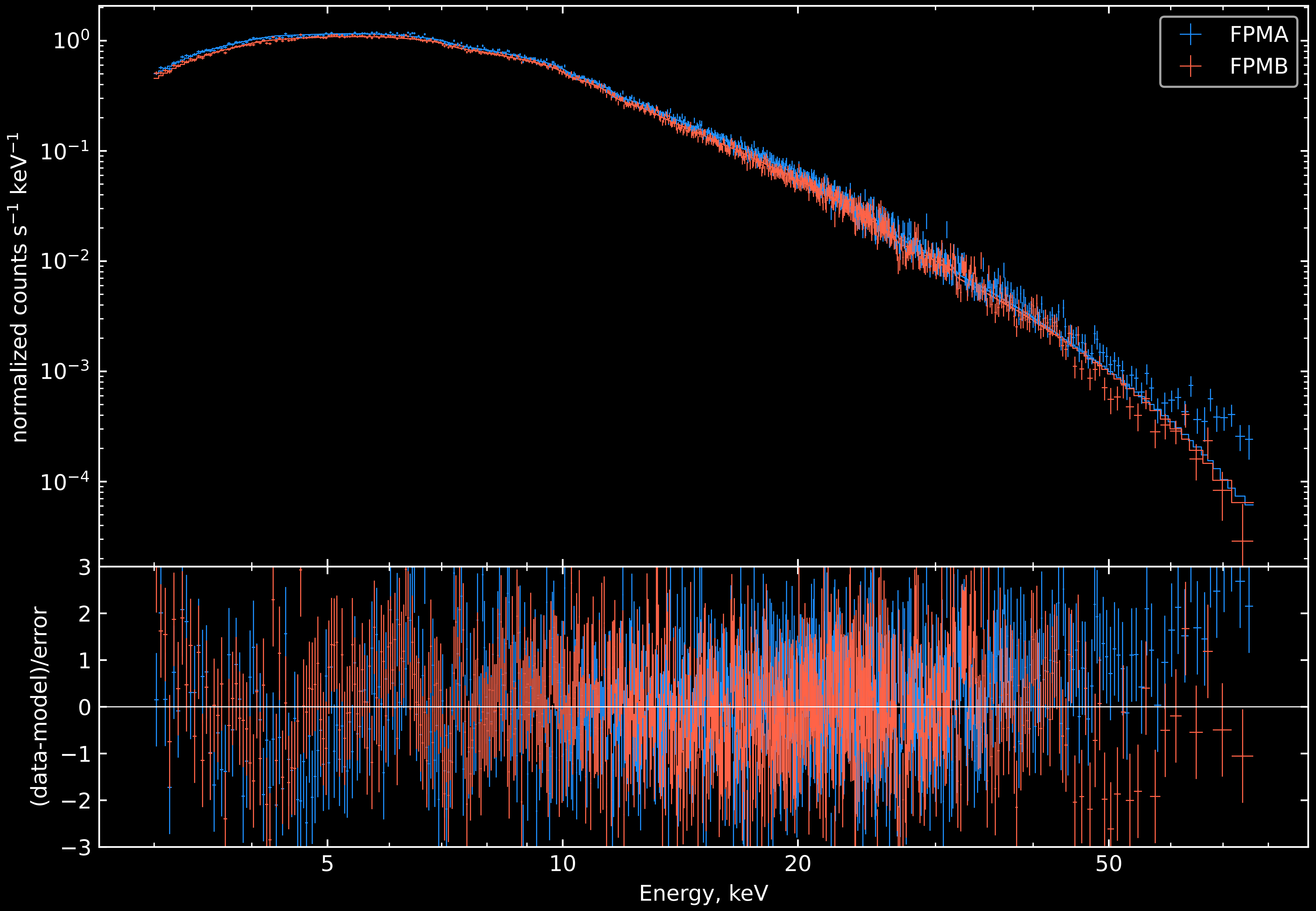

`tbabs*highecut*pow`

$N_H = (8.3^{+0.4}_{-0.6}) \times 10^{22}$ cm^{-2}

$E_C = 7.2^{+0.3}_{-0.6}$ keV

$E_F = 26^{+1}_{-2}$ keV

$\Gamma = 1.65^{+0.28}_{-0.57}$

$$L_{bol} = (1.6^{+0.5}_{-0.7}) \times 10^{36} \text{ erg s}^{-1} < L_{crit} = 4 \times 10^{36} \text{ erg s}^{-1}$$

Bayesian blocks
Flare peaks
Light curve
Rate, counts/s
Time, s
20
40
60
80
11500
12000
12500
13000
13500
14000
14500
15000

$v_w \approx 1700$ km s^{-1} inconsistent with RSG wind velocities ($\sim 10 - 30$ km s^{-1})

Results

Astronomy Letters, 2023, Vol. 49, No. 5

Spectral and temporal analysis of the Supergiant Fast X-ray Transient IGR J16195-4945 with SRG/ART-XC

M. N. Satybaldiev*[1,2], I. A. Mereminskiy[1], A. A. Lutovinov[1], D. I. Karasev[1], A. N. Semena[1], A. E. Shtykovsky[1]

[1] *Space Research Institute, Moscow*
[2] *Moscow Institute of Physics and Technology*

Received 28.03.2023. Revised 19.05.2023. Accepted 03.06.2023.

https://ui.adsabs.harvard.edu/abs/2023AstL...49..249S/abstract

- spectral and temporal analysis of IGR J16195-4945 and 3A 1954+319
- IGR J16195-4945 shows “colorless” X-ray variability
- flare properties of IGR J16195-4945 are consistent with subsonic settling accretion model and with other SFXTs
- no pulsations detected in IGR J16195-4945 data
- IGR J16195-4945 wind velocity estimated $v_w \approx 500$ km s^{-1}
- IGR J16195-4945 exhibits unusual rapid IR variability
- 3A 1954+319 flare properties are different from SFXTs
- 3A 1954+319 wind velocity estimation is too high for red supergiants

Thank you!

Orbital folded light curve of IGR J16195-4945(Cusumano et al., 2016)

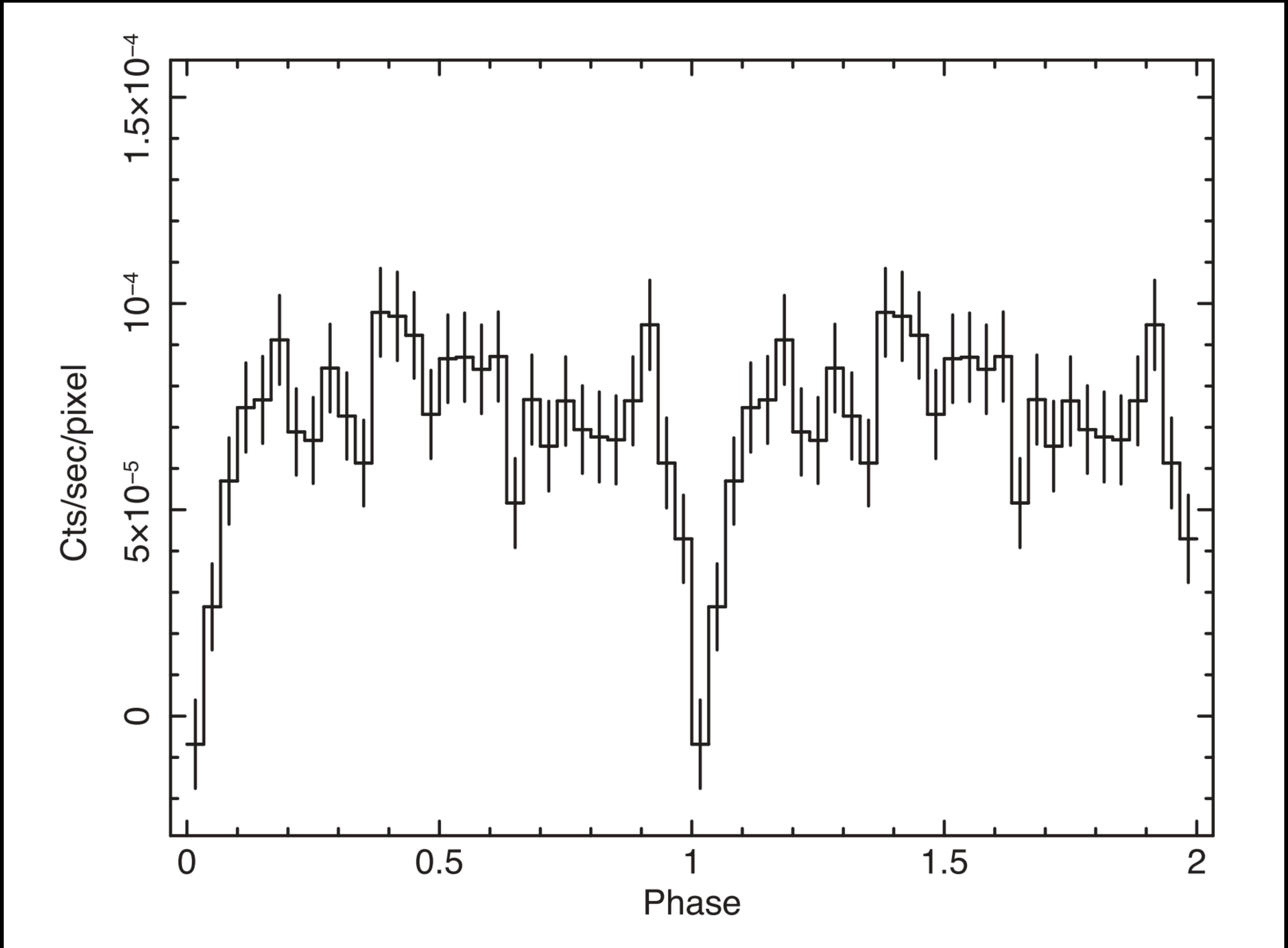

Table 1. Parameters of the best-fit for the spectra of IGR J16195-4945

Segment	N_H, cm^{-2}	Γ	E_{cut}, keV	χ^2 / d.o.f.	F[4-20 keV], erg s^{-1} cm^{-2}
Full ART-XC + XRT + BAT	$(12 \pm 2) \times 10^{22}$	0.56 ± 0.15	13 ± 2	231.29 / 185	$(2.5 \pm 0.1) \times 10^{-11}$
ART-XC	31 ± 15	1.09 ± 0.41	19^{+28}_{-7}	191.15 / 157	$(2.9^{+0.4}_{-0.2}) \times 10^{-11}$
Full ART-XC (fixed N_H)	12×10^{22}	0.67 ± 0.27	15^{+12}_{-5}	196.49 / 158	$(2.4 \pm 0.3) \times 10^{-11}$
ART-XC: ACG (fixed N_H)	12×10^{22}	$0.58^{+0.84}_{-0.97}$	10^{+88}_{-5}	187.16 / 158	$(0.9 \pm 0.1) \times 10^{-11}$
ART-XC: BDF (fixed N_H)	12×10^{22}	0.59 ± 0.27	15^{+9}_{-5}	184.15 / 158	$(4.1 \pm 0.2) \times 10^{-11}$

Table 2. Measured flare properties

#	Energy, 10^{38} erg (1-10 keV)	Waiting time, s	Duration, s	Rise time, s	Pre-flare L_x, 10^{34} erg s^{-1} (1-10 keV)
1	4.4 ± 0.2	15000(*)	4000	2500	1.6 ± 0.1
2	5.9 ± 0.3	8500	5500	2500	4.0 ± 0.2
3	3.1 ± 0.3	6250	2000	500	5.5 ± 0.3
4	3.5 ± 0.2	4750	4500	1500	5.4 ± 0.4
5	4.1 ± 0.2	15750	5000	1500	2.6 ± 0.1
6	3.4 ± 0.2	15500	3000	2000	4.3 ± 0.2

tions have the form: flare waiting time ΔT on pre-flare luminosity ($L_{\rm X,pre}$, pre-flare):

$$\Delta T \approx 130[\mathrm{s}]\left(\frac{\alpha}{0.03}\right)A\zeta^{2/9}\mu_{30}^{2/3}\dot{M}_{16}^{-1},$$

energy released in a flare ΔE on its duration Δt:

$$\Delta E \approx 3\times10^{35}[\mathrm{erg\ s^{-1}}]\left(\frac{\alpha}{0.03}\right)A\zeta^{2/9}\mu_{30}^{2/3}v_8^3\Delta t,$$

flare rise time δt_{rise} on $L_{\rm X,pre}$:

$$\delta t_{rise} \simeq 30[\mathrm{c}]\zeta^{4/27}\mu_{30}^{7/9}\dot{M}_{16}^{-2/3},$$

ratio between the flare energy and the waiting time $\Delta E/\Delta T$:

$$\frac{\Delta E}{\Delta T} = 10^{36}[\mathrm{erg\ s^{-1}}]\dot{M}_{16},$$

where the mass accretion rate $\dot{M}_X = 10^{16}[\mathrm{g\ s^{-1}}]\dot{M}_{16}$ related to pre-flare luminosity as $L_{\rm X,pre} = 0.1\dot{M}_X c^2$, $\alpha \sim 0.03$ - , the dimensionless factor, defining the non-linear growth rate , $A \lesssim 1$ is the effective Atwood number, $\zeta \lesssim 1$ characterizes the size of the RTI region in units of the magnetospheric radius R_m, $\mu = 10^{30}[\mathrm{G\ cm^3}]\mu_{30}$ - the NS magnetic moment, $v = 10^8[\mathrm{cm\ s^{-1}}]v_8$ - the relative wind velocity.

$$\Delta t \approx 400[\mathrm{s}]\left(\frac{v_w}{1000[\mathrm{km\ s^{-1}}]}\right)^{-3}$$

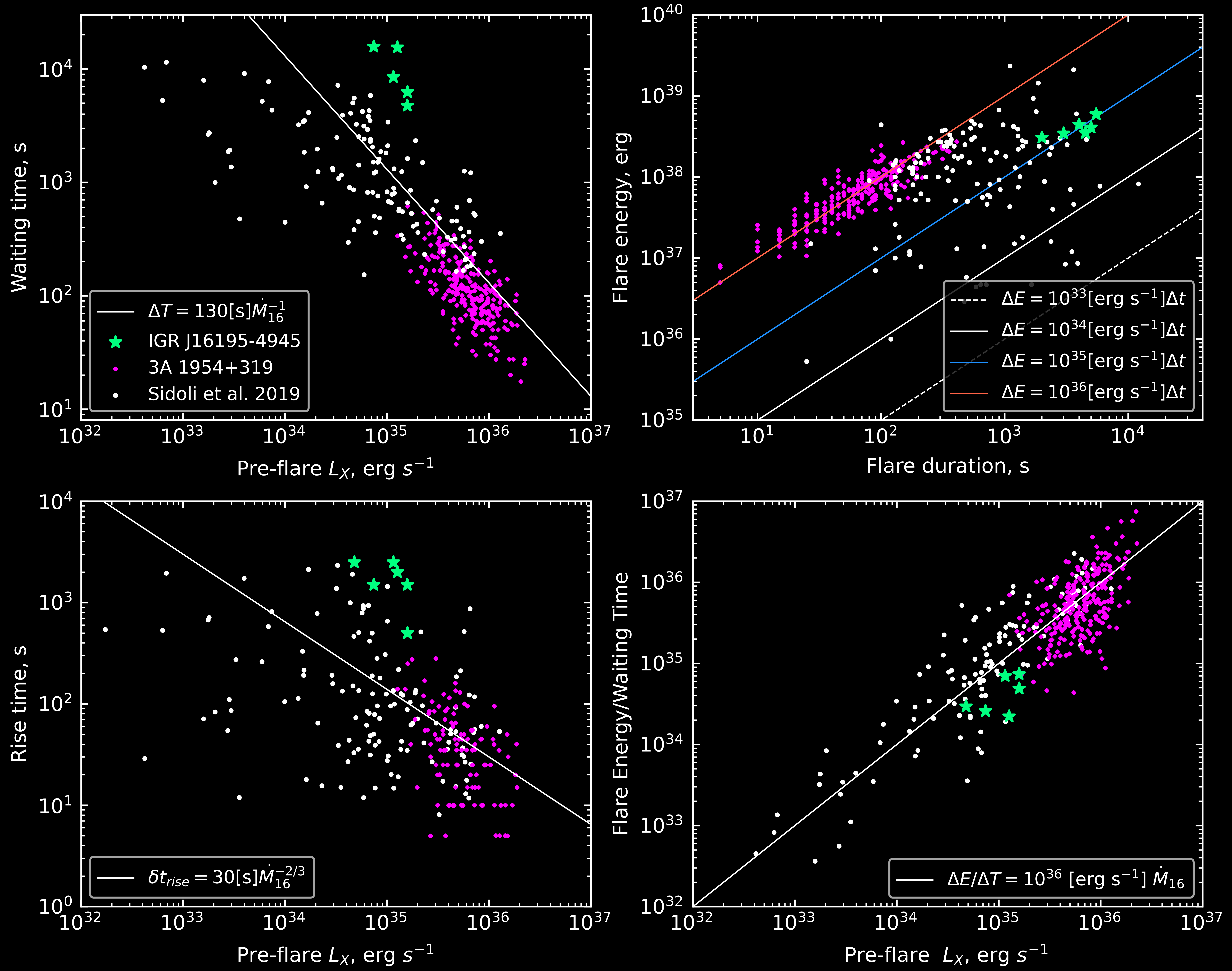

Waiting time, s
Pre-flare L_X, erg s^{-1}
$\Delta T = 130[\mathrm{s}]\dot{M}_{16}^{-1}$
IGR J16195-4945
3A 1954+319
Sidoli et al. 2019
Flare energy, erg
Flare duration, s
$\Delta E = 10^{33}[\mathrm{erg\ s^{-1}}]\Delta t$
$\Delta E = 10^{34}[\mathrm{erg\ s^{-1}}]\Delta t$
$\Delta E = 10^{35}[\mathrm{erg\ s^{-1}}]\Delta t$
$\Delta E = 10^{36}[\mathrm{erg\ s^{-1}}]\Delta t$
Rise time, s
$\delta t_{rise} = 30[\mathrm{s}]\dot{M}_{16}^{-2/3}$
Flare Energy/Waiting Time
$\Delta E/\Delta T = 10^{36}\ [\mathrm{erg\ s^{-1}}]\ \dot{M}_{16}$

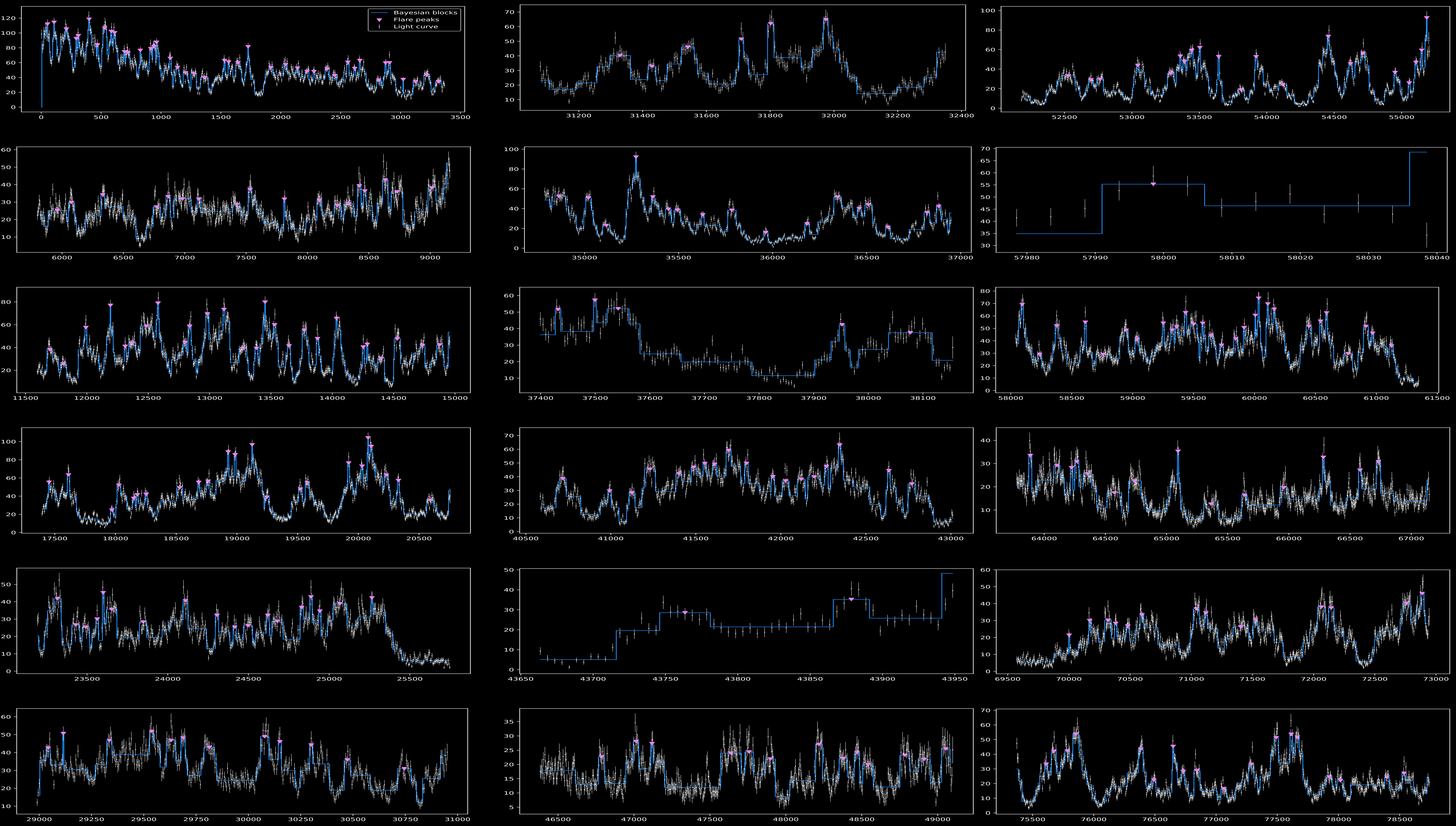

Bayesian blocks
Flare peaks
Light curve

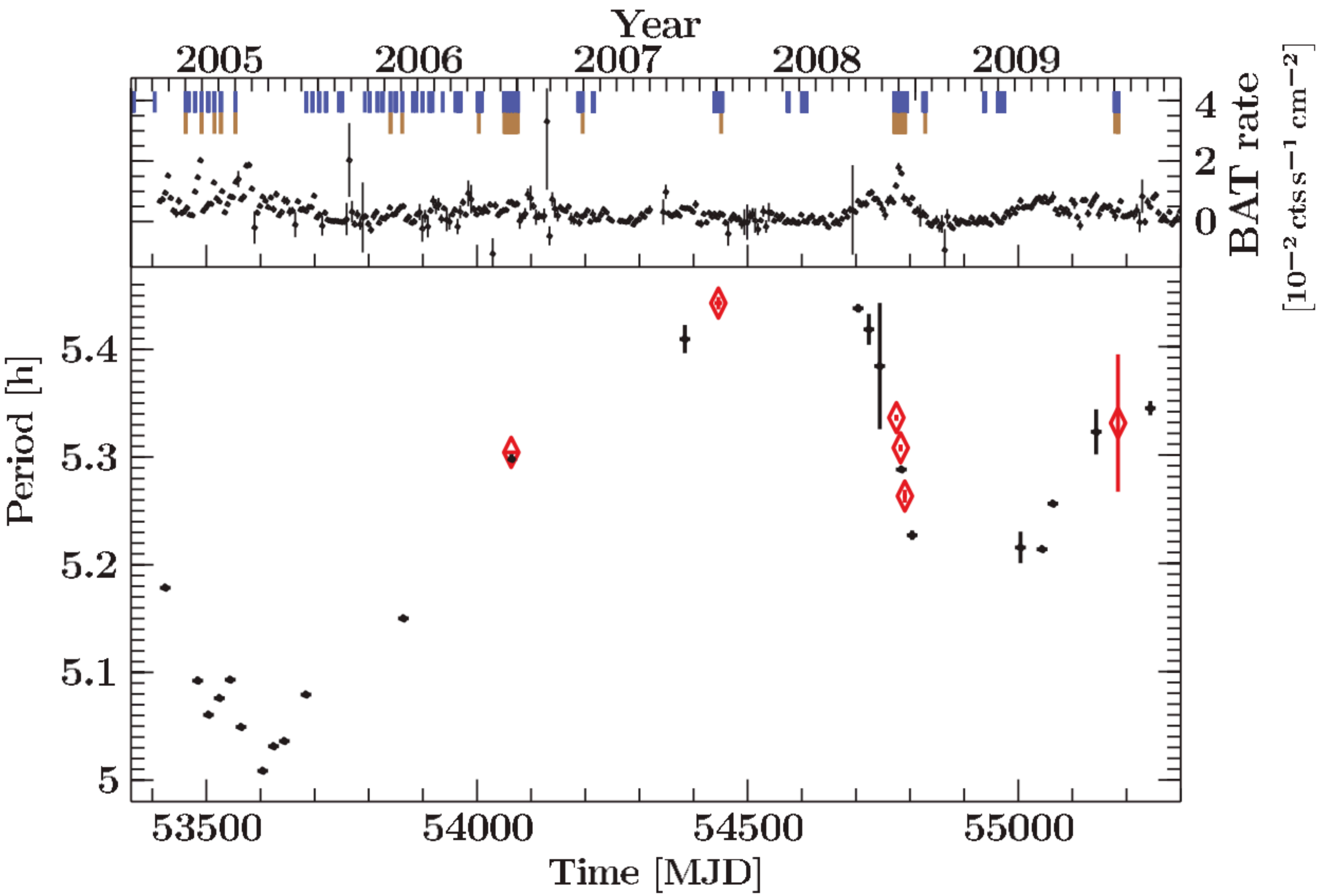

Figure 1. From top to bottom: *INTEGRAL* observations of 3A 1954 + 319 with an offset angle ⩽10° and *INTEGRAL*-ISGRI detections (blue and brown tickmarks, respectively). The long-term light curve shown was obtained by *Swift*-BAT in the 15–50 keV range and has been rebinned to a resolution of 5 days. The lower part of the figure shows the pulse period evolution as determined by BAT (black) and ISGRI (red).

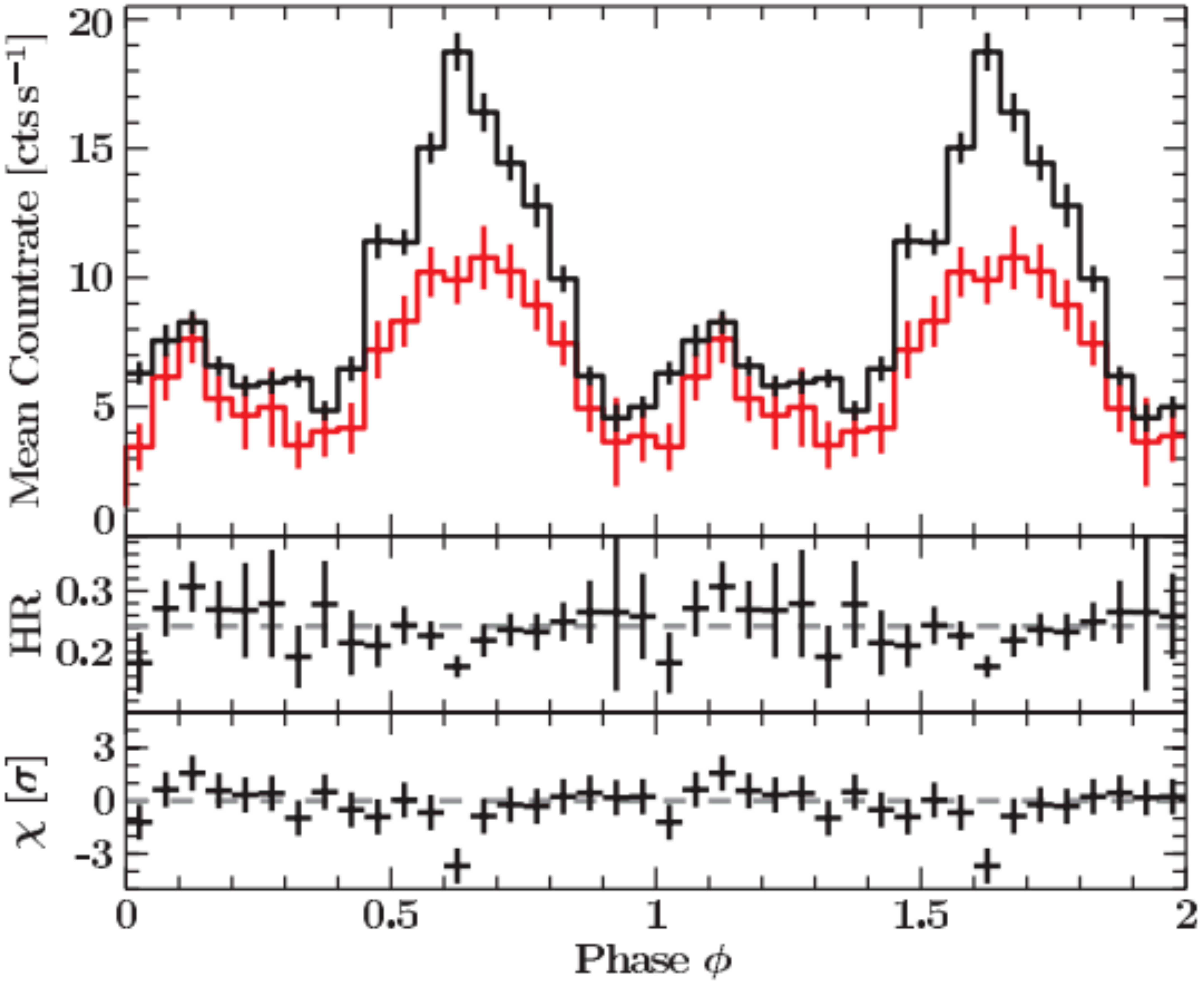

Figure 3. Upper panel: ISGRI pulse profiles for the flaring episode in 2008, in the energy ranges of 20–40 keV (black) and 40–100 keV (red, multiplied by 3 for better visibility). Middle panel: hardness ratio obtained by dividing the 40–100 keV by the 20–40 keV profile. The dashed line indicates the mean hardness. Lower panel: deviation of the hardness ratio from the mean hardness in units of σ. The dashed line indicates no deviation.

Marcu et al. 2011